

New Orientifold Weak Coupling Limits in F-theory

Paolo Aluffi♣ and Mboyo Esole♠

♣ Mathematics Department, Florida State University, Tallahassee FL 32306, U.S.A.

♠ Jefferson Physical Laboratory, Harvard University, Cambridge, MA 02138, U.S.A.

Abstract

We present new explicit constructions of weak coupling limits of F-theory generalizing Sen's construction to elliptic fibrations which are not necessary given in a Weierstrass form. These new constructions allow for an elegant derivation of several brane configurations that do not occur within the original framework of Sen's limit, or which would require complicated geometric tuning or break supersymmetry. Our approach is streamlined by first deriving a simple geometric interpretation of Sen's weak coupling limit. This leads to a natural way of organizing all such limits in terms of transitions from semistable to unstable singular fibers. These constructions provide a new playground for model builders as they enlarge the number of supersymmetric configurations that can be constructed in F-theory. We present several explicit examples for E_8 , E_7 and E_6 elliptic fibrations.

*He thought he saw a Platypus
Descending from a train:
He looked again, and found it was
A split D7-Brane.
'So sad, alas, so sad!' he said,
'That all has been in vain!'¹*

♣aluffi@math.fsu.edu

♠esole@physics.harvard.edu

¹From Matilde Marcolli, *The Mad String Theorist's Song*.

CONTENTS

1. Introduction	2
1.1. Sen's weak coupling limit	3
1.2. The need for new weak coupling limits	5
1.3. Moving away from Weierstrass models	6
1.4. Geometrization of Sen's weak coupling limit	7
1.5. Consistency check	8
1.6. Topological results inspired by tadpole relations	9
1.7. E_8, E_7, E_6 families of elliptic fibrations	9
1.8. Examples of new weak coupling limits	10
1.9. Singularities and the weak coupling limit of F-theory	14
2. Families of elliptic fibrations and their singular fibers	14
2.1. Singularities of E_7 fibrations	16
2.2. Singularities of E_6 fibrations	18
2.3. Semistable and unstable fibers	22
3. Weak coupling limits	22
3.1. Sen's limit, revisited	23
3.2. The strategy	25
3.3. Two E_7 weak coupling limits	25
3.4. An E_6 weak coupling limit	27
3.5. Discussion	29
4. Tadpole relations	30
4.1. F-theory-type-IIB tadpole matching condition	30
4.2. Sethi-Vafa-Witten formulas	32
4.3. Euler characteristic and Chern class identities	34
4.4. A classification of configurations of smooth branes	38
5. A visit to the zoo	40
5.1. E_8 limits	40
5.2. E_7 limits	41
5.3. E_6 limits	42
6. Conclusions and discussions	43
References	45

1. INTRODUCTION

Type IIB string theory is an interesting framework for model building in view of the possibility to stabilize moduli. F-theory was introduced by Cumrun Vafa [1] and provides an elegant geometric formulation of non-perturbative IIB string theory in the presence of 7-branes and D3 branes [1, 2, 3]. An F-theory compactification requires an elliptic fibered space $Y \rightarrow B$ over the compact space B on which the dual type IIB theory is compactified. The elliptic fiber is a two-torus whose complex structure is interpreted as the type IIB axion-dilaton field. The modular transformations of the elliptic fiber are a geometric realization of type IIB S-duality transformations. Around a singular fiber, the monodromy of the axion-dilaton field characterizes the non-perturbative (p, q) -seven-branes [4, 5, 6, 7, 8]. An F-theory approach to type IIB model building brings more constraints coming from its non-perturbative origin. The type and number of branes, the gauge group and the D3 tadpole are all determined by the geometry of the elliptic fibration and particularly by the type of singular fibers. The location of the 7-branes is given by the *discriminant locus*: the locus of all singular fibers in the base. Each irreducible component of the discriminant locus corresponds to a (p, q) -brane. In the case of F-theory compactified on elliptically fibered four-folds, the D3 tadpole is given by the Euler characteristic of the four-fold divided by 24 [9]. For a review on F-theory type IIB model building we refer to [10, 11].

Several realistic features of particle phenomenology seem to emerge naturally in the context of local models in F-theory where gravity is decoupled [12, 13, 14]. For reviews on local model building in F-theory, we refer to [14, 15, 16, 17]. The main shortcoming of local model building is that it does not keep track of all the global consistency conditions required by the full string theory. For example, the tadpole cancellation conditions are usually not addressed. Recently, there have been several attempts to reconcile the results of local model building with all the global constraints coming from F-theory on compact manifolds [11, 18, 19, 20, 21, 22]. In this context, defining the weak coupling limit of F-theory is a crucial step. So far, Sen's weak coupling limit of F-theory was the only option available [23].

The goal of this paper is to develop new ways of taking the weak coupling limit of F-theory, generalizing Sen's technique to other families of elliptic fibrations. The results obtained here can also be read 'backwards' as providing new F-theory lifts for type IIB orientifold compactifications. Interestingly, the new weak coupling limits presented here avoid several inherent complications of Sen's limit of a Weierstrass model. In particular, we can avoid the singularities of the D7 divisors that are characteristic of Sen's weak coupling limit [24, 25, 26]. We also propose F-theory constructions that satisfy some important topological relations required by the consistency of the duality between type IIB and F-theory [24, 25]. This is done in situations where the same relation would inevitably be violated or would require turning on fluxes that would break supersymmetry in the context of Sen's limit of a Weierstrass model. For example, we present F-theory engineering of brane-image-brane configurations that do not break supersymmetry through the violation of D-term constraints in contrast to a typical brane-image-brane configuration resulting from the usual Sen's limit as explained in §4.4 of [25].

The structure of this paper is as follows. In the rest of the introduction, we review the physics of Sen's weak coupling limit of F-theory and we introduce the main ideas behind the

constructions presented in this paper. In particular, we discuss the geometrization of Sen's limit and motivate the introduction of new families of elliptic fibrations. As an illustration, we discuss the physics of some explicit examples constructed in this paper that would suffer from several difficulties in the usual Sen's limit. In section 2, we define the new families of elliptic fibrations we will consider in the paper and study systematically their singular fibers. In section 3 we derive the new weak coupling limits for the families introduced in section 2. In section 4 we prove a compact generalization of Sethi-Vafa-Witten formula to compute the Euler characteristic of an elliptic fibration in terms of its base, and we analyze the topological relation induced by the matching between the D3 tadpole in F-theory and in type IIB in the absence of fluxes. Inspired by the physics, we can prove more general relations, valid without any restriction on the dimension of the elliptic fibration and without imposing the Calabi-Yau condition. In section 5 we provide a list of weak coupling limits for E_8 , E_7 and E_6 elliptic fibrations. Finally we conclude with a discussion in section 6.

1.1. Sen's weak coupling limit. In the weak coupling limit of F-theory, one obtains a type IIB theory with with O7 orientifold planes in order to cancel the D7 tadpole. In the weak coupling limit of F-theory, Ashoke Sen has provided the only systematic way to derive a type IIB orientifold limit of F-theory in the familiar case of elliptic fibrations given by a Weierstrass model [23]. For reasons that we will explain later, we refer to the Weierstrass model as an E_8 -fibration. Its defining equation is

$$E_8 : y^2 = x^3 + Fxz^6 + Gz^6,$$

where F and G are respectively sections of \mathcal{L}^4 and \mathcal{L}^6 , where \mathcal{L} is a line bundle over the base B . In the case of a Calabi-Yau elliptic fibration, we have $c_1(B) = c_1(\mathcal{L})$. A Weierstrass model admits a discriminant $\Delta = 4F^3 + 27G^2$ whose vanishing locus determines the location of singular fibers. There are essentially two types of singular fibers: the general element of the discriminant locus $\Delta = 0$ is a nodal curve; when $F = G = 0$, the nodal curve specializes to a cuspidal curve. Sen's limit is given by the expression

$$F = -3h^2 + C\eta, \quad G = -2h^3 + Ch\eta + C^2\chi.$$

At leading order, the discriminant and the j -invariant are

$$\Delta \sim h^2(\eta^2 + 12h\chi), \quad j \sim \frac{h^4}{C^2(\eta^2 + 12h\chi)}.$$

One can construct a Calabi-Yau 3-fold which is a double cover of the base:

$$X : \xi^2 = h,$$

and the involution is given by $\sigma : X \rightarrow X : \xi \mapsto -\xi$. The orientifold involution is then $\Omega\sigma(-)^{F_L}$, where Ω is the world-sheet orientation reversal and F_L is the space-time fermion number from the left-moving sector of the world-sheet. The orientifold plane in X is $O : \xi = 0$ while in the base it was given by $\underline{O} : h = 0$. The D7 locus in the base was $\underline{D} : \eta^2 + 12h\chi = 0$ while in X it is given by $D : \eta^2 + 12\xi^2\chi = 0$.

The physics of Sen's limit has been explored recently in several papers [24, 26, 25, 27, 28, 29]. We would like to emphasize the following properties [25, 24, 26]:

- An orientifold seven plane is a perturbative object. It splits into two non-perturbative (p, q) -branes as the coupling becomes stronger [23].

- The locus of the D7 brane $D : \eta^2 + 12\xi^2\chi = 0$ is singular along the locus $\eta = \xi = 0$ of double points and the singularity worsens on the pinch locus $\eta = \xi = \chi = 0$. Near each of these pinch points, we can use η, χ and ξ as local coordinate and the surface wrapped by the D7 brane looks like a Whitney umbrella $D : \eta^2 + 12\xi^2\chi = 0$. We will refer to such a singular D7-brane as a *Whitney D7-brane*. The presence of the singularities forces one to carefully define the Euler characteristic used to compute the induced D3 charge [24, 25].
- A brane-image-brane pair is just a specialization of a Whitney D7-brane $u^2 - v^2w = 0$ when w is a perfect square; if $12\chi = \psi^2$, then D splits as $D = D_+ + D_-$ with $D_{\pm} : \eta \pm \xi\psi = 0$. In the base, the equation of a Whitney D7-brane is $\underline{D} : \eta^2 + 12h\chi = 0$, which specializes to $\underline{D} : \eta^2 + h\psi^2 = 0$ for a brane-image-brane pair. Interestingly, in the base, a brane-image-brane pair has the structure of a Whitney umbrella ($u^2 - v^2w = 0$ in \mathbb{C}^3) whereas a Whitney brane has the structure of a cone ($u^2 - vw = 0$ in \mathbb{C}^3).
- The D7 branes appearing in limit always have a double intersection (or more generally an intersection with even multiplicity) with an orientifold seven plane. This double intersection property is a direct consequence of the Whitney umbrella geometry in Sen's limit [25, 26]. Indeed, as $\xi = 0$, we get $\eta^2 = 0$. More generally, it can be seen as a consequence of Dirac quantization in the case of $O7^-$ plane [25].
- D3 branes being S-duality invariant, the D3 tadpole does not depend on the string coupling. Therefore, one would expect to find a matching between the F-theory and the type IIB prediction of the D3 tadpole. In F-theory, the D3 tadpole is given by the Euler characteristic of the elliptic fibration. In type IIB, the D3 tadpole admits contributions coming from the induced D3 charge of seven branes and orientifold planes. In the absence of fluxes, this leads to a *F-theory/Type IIB tadpole matching condition* [24, 25]:

$$2\chi(Y) \stackrel{?}{=} 4\chi(O) + \chi(D).$$

As stated, this condition is not verified in Sen's limit, and in other similar situations. In cases where the Euler characteristic of the four-fold overshoots² the contribution from orientifold planes and D7 branes, one could compensate by turning on world-volume fluxes on the compact surfaces wrapped by the seven branes [25]. In the case of Sen's limit, if the D7 were wrapping a smooth locus one would find an induced D3 brane in type IIB that would on the contrary overshoot the F-theory prediction. This mismatch could not be corrected by turning on world volume fluxes, since they would only contribute positively to the induced D3 tadpole and therefore worsen the discrepancy. However, in Sen's limit the D7 brane wraps a singular hypersurface, and the correct notion of Euler characteristic for such a locus is open to interpretation. As shown in [24], the tadpole matching condition is satisfied in Sen's limit for an appropriate Euler characteristic χ_o , where the singularities provide a contribution taking care of the discrepancy. This Euler characteristic $\chi_o(D)$ was introduced in [24, 25]. It satisfies all the physics tests as shown in [25]. Mathematically it can be defined as the Euler characteristic of a normalization of the singular surface D , corrected by the contribution from the pinch locus [24]. This can be understood as a generalization of the stringy Euler characteristic [24].

²In these considerations we implicitly assume that $\dim B = 3$ and $c_1(B)^3 > 0$, for simplicity.

- In the context of Sen's weak coupling limit of a Weierstrass model, there is in general only one D7 brane located on an irreducible locus. There are also smooth specializations, such as the brane-image-brane pairs; these configurations naturally satisfy the double intersection property of 7-branes and orientifold since the brane and its image brane always meet on the orientifold. However, without fluxes, they always leads to a type IIB D3 induced tadpole which is lower (for a base B of dimension 3, and $c_1(B)^3 > 0$) than the one expected from F-theory. Therefore, they always require the presence of world volume fluxes. Since the world volume fluxes also contribute to the D5 brane charges but are odd under the orientifold involution, they gives different central charges for the brane on D_+ and its image-brane on D_- . This leads to a breaking of supersymmetry since the D-term constraints are not respected [25].

1.2. The need for new weak coupling limits. The previous review of the physics of Sen's weak coupling limit of a Weierstrass model (an E_8 -elliptic fibration) immediately raises the question of its uniqueness, for the following reasons. Although it is well appreciated that F-theory adds severe constraints to type IIB theory, Sen's limit reduces very drastically the number of allowed configurations. It also implies that some very simple configurations in type IIB (like the brane-image-brane configuration) are generally non-supersymmetric. The presence of the Whitney umbrella singularity makes it more difficult to geometrically engineer specific configurations of intersecting branes in the context of Sen's limit. We consider all these limitations as an open invitation to find new weak coupling limits. The non-uniqueness of Sen's weak coupling limit can already be appreciated within the original framework of a Weierstrass model. Consider for example the limit

$$F = -3h^2 + C\eta, \quad G = -2h^3 + C(h\eta + \chi).$$

It leads to

$$\Delta \sim Ch^3\chi, \quad j \sim \frac{h^3}{C\chi}.$$

This corresponds to a bound state of an orientifold $O : \xi = 0$ with a brane-image-brane on top of it ($D_{\pm} : \pm\xi = 0$) together with a brane on a smooth locus $D : \chi = 0$. Since D_{\pm} have the same Euler characteristic as the orientifold plane, the F-theory-type- IIB D3 tadpole matching gives in the absence of fluxes:

$$2\chi(Y) \stackrel{?}{=} 6\chi(O) + \chi(D).$$

This relation does not hold. We also note that D does not have a double intersection with the orientifold plane. Each time it intersects the orientifold plane, it also intersects the two D7 branes located on O , in total we have an odd number of D7 contributions.

The study of more sophisticated configurations within the Weierstrass model quickly leads to complicated expressions that seem completely unmotivated and arbitrary. This seems to indicate that we might win some intuition and simplicity by considering new weak coupling limits that do not arise from smooth Weierstrass models. In the context of Sen's weak coupling limit of F-theory with Weierstrass models, new methods with direct applications to model building have been developed recently by Andres Collinucci[28, 29]. The same ideas can be applied to the new weak coupling limits of F-theory we construct in this paper.

1.3. Moving away from Weierstrass models. A smooth elliptic curve is a curve of genus one (with a marked point). While curves of genus zero are all isomorphic to a two sphere (a \mathbb{CP}^1), curves of genus one are classified by a complex parameter which controls their complex structure. This is expressed by the j -invariant of the elliptic curve. Two curves of genus one are isomorphic if and only if they have the same j -invariant. The study of elliptic curves and elliptic fibrations is often simplified by the following two properties:

- Every smooth elliptic curve is isomorphic to an elliptic curve written in Weierstrass form.
- Every elliptic fibration is birationally equivalent to a Weierstrass model.

When we consider an elliptic fibration which is not in Weierstrass form, it can be useful to know exactly the Weierstrass form of a birationally equivalent elliptic fibration. This is because there are important properties of the elliptic fibration that could be computed more simply in certain birationally equivalent elliptic fibrations, and particularly in a birationally equivalent Weierstrass model. Two important examples are the location of the singular fibers and the j -invariant of an elliptic fiber, which may be computed by using the Weierstrass model. Because of this, it is often believed that it is in fact enough to consider only Weierstrass models in F-theory. However, this can only be done at the price of a desingularization process that may be difficult to handle. The Weierstrass model *per se* does not preserve all physically relevant quantities of a fibration: for example, the type of singular fibers of a fibration is only recoverable from the Weierstrass model through a local analysis of the equation and of its discriminant (by Tate's algorithm, see [34]), not directly from the model itself.

In the case where the elliptic fibration is a four-fold, the topology of the singular fibers plays a central role in F-theory since it determines the Euler characteristic of the elliptic fibration and therefore the F-theory D3 tadpole. The Euler characteristic of an elliptic fibration gets contributions only from singular fibers. A birational transformation can change the type of singular fibers and therefore change the Euler characteristic of the elliptic fibration³. For compactifications on four-folds, this leads to a different prediction for the D3 tadpole and therefore it changes the physics.

Once we consider elliptic fibrations which are not in Weierstrass form, their Euler characteristic can be lower⁴ than the Euler characteristic of a smooth Weierstrass model defined on the same basis, with respect to the same line bundle. In particular, it is possible to accommodate brane-image-brane configurations that do not require turning on fluxes to satisfy the F-theory-type IIB tadpole matching condition. It follows that such brane-image-brane configurations would not break supersymmetry in contrast to those obtained as special configurations of Sen's limit in a Weierstrass model. This illustrates the fact that restricting ourselves to the Weierstrass model reduces artificially the number of consistent compactifications allowed in F-theory. As an illustration, we will show that for the fibrations that we consider in this paper there are in general only six possible configurations of branes wrapping smooth divisors in a Calabi-Yau and satisfying the F-theory-type-IIB tadpole matching condition. Only one of these six configurations is in a Weierstrass model, and this

³While smooth birationally equivalent Calabi-Yau varieties have the same Euler characteristic, [31], and even commensurable Chern classes, [32, 33], we note that even in the Calabi-Yau case the Weierstrass model of a smooth elliptic fibration may be singular; the Euler characteristic should be expected to change in this case.

⁴See footnote 2.

j -invariant	(elliptic) curve	condition
$j < \infty$	smooth	$\Delta \neq 0$
$j = \infty$	singular and semistable	$\Delta = 0, F, G \neq 0$
$j = \frac{0}{0}$	singular and unstable	$F = G = 0$

TABLE 1. Types of fibers of elliptic fibrations.

configuration is not yet realized as a weak coupling limit of F-theory. Moreover, the allowed configurations reduce to three if we do not insist on the Calabi-Yau condition, and none of these three configurations is realized in a Weierstrass model. This is reviewed further in the introduction and proved in §4.4.

1.4. Geometrization of Sen’s weak coupling limit. In our investigation of weak coupling limits, a geometric picture quickly emerges. It is based on the classification of semistable and unstable singular fibers of an elliptic fibration. In the case of curves of genus one, semistable and unstable curves are simply defined by the two possible behaviors of the j -invariant: it can be infinite or undetermined of type $\frac{0}{0}$. When it is infinite, we have a (singular) *semistable fiber* and when it is undetermined, it corresponds to an *unstable fiber*.

Since the j -invariant is a birational invariant, it can be computed without any loss of generality in a Weierstrass model birationally equivalent to the elliptic fibration we consider. The singular fibers are located on the discriminant $\Delta = 4F^3 + 27G^2$. The smooth fibers are such that $\Delta \neq 0$. Since the singular fibers are characterized by $\Delta = 0$ and the j -invariant is

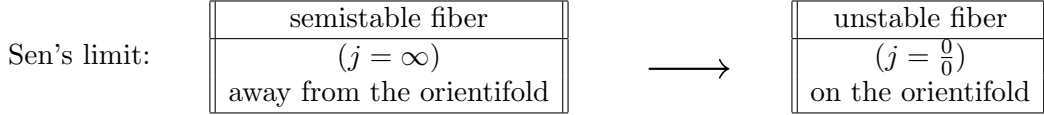
$$j \sim \frac{F^3}{\Delta},$$

we see that the semistable singular fibers are characterized by $\Delta = 0, F, G \neq 0$ while the singular unstable fibers are given by $F = G = 0$. It follows that an unstable fiber is a cuspidal curve, and the set of unstable fibers ($F = G = 0$) is the closure of the cuspidal locus. Its defining characteristic is that this is the locus of fibers having an undefined j -invariant of type $\frac{0}{0}$. They consist of cuspidal curves and their specializations. The general semistable singular fiber is a nodal curve, but it can specialize to other types of curves that are not a specialization of a cusp.

In terms of the complex structure of the elliptic curve, the j -invariant is expressed as

$$j(q) = 744 + \frac{1}{q} + \sum_n d_n q^n, \quad q = \exp(2\pi i\tau), \quad d_n \in \mathbb{N}.$$

Here $\tau = a + ie^\varphi$ determines the complex structure of the elliptic curve. In F-theory, it is the axion-dilaton field. In particular, its imaginary part, namely $e^\varphi = \frac{1}{g_s}$ is the inverse of the string coupling g_s . The module of $q = \exp(2\pi i\tau)$ is $|q| = g_s^{2\pi}$. It follows that when we go to the weak coupling limit ($g_s \rightarrow 0$), the j -invariant is dominated by its pole $\frac{1}{q}$ and goes to infinity. However, as we will see in §3.5, as we reach the orientifold plane the j -invariant is undetermined, of the form $\frac{0}{0}$. It follows that *the weak coupling limit singles out semistable singular fibers away from the orientifold and specializes to an unstable fiber on the orientifold locus*. A weak coupling limit analogous to Sen’s always defines a transition from a semistable singular fiber (away from the orientifold) to an unstable singular fiber (on the orientifold plane).



1.4.1. *Geometric classification of weak coupling limits.* The observation that a weak coupling limit is characterized by a transition from a semistable singular fiber to an unstable one is the basis for our strategy to construct weak coupling limit of a given elliptic fibration:

- We choose a family of elliptic fibrations.
- We classify all singular fibers of the elliptic fibration.
- We determine those that are semistable and those that are unstable.
- Each specialization “semistable \rightarrow unstable” leads to a family potentially yielding a weak coupling limit.

1.5. **Consistency check.** In our investigation of orientifold weak coupling limits of F -theory, we will always check if the following properties are realized:

- Existence of a smooth Calabi-Yau double cover of the base. This will be done by restricting the orientifold divisor $h = 0$ to be a section of an appropriate line bundle over the base [23]. However, we will work with elliptic fibrations of arbitrary dimension and we will not restrict ourself to Calabi-Yau spaces. We will denote by O the orientifold plane and by D_j the D7 branes⁵. When we refer to their location in the base rather than in the double cover, we underline $(\underline{O}, \underline{D}_j)$ their notation.
- Vanishing of the D7 tadpole: the sum of class of the orientifold planes is 8 times the sum of all the D7 branes when computed in the double cover:

$$8[O] = \sum_i [D_i].$$

- F-IIB matching of the D3 tadpole in the absence of fluxes. As a non-trivial check of the consistency of the new weak coupling limits, we study the matching of the F-theory and type IIB D3 tadpole in the absence of fluxes. This leads to a non-trivial topological relation among the Euler characteristics of the varieties involved in the construction [24, 25]:

$$2\chi(Y) = 4\chi(O) + \sum_j \chi(D_j).$$

In particular, in the presence of brane-image-branes, this condition will ensure that there is no need to add brane fluxes and therefore we avoid the usual breaking of supersymmetry by a violation of the D-term constraints. When a D7 brane wraps a singular variety, we use the Euler characteristic χ_o , that is the Euler characteristic of its normalization corrected by a contribution from the pinch locus.

- D7 branes always intersect the orientifold plane with even multiplicity in order to avoid a violation of the Dirac quantization [25]. We will not impose this on the construction, but we will observe that it always occurs.

⁵To avoid an awkward notation, we will refer to these as $D7$ branes even when working over a base of arbitrary dimension.

1.6. Topological results inspired by tadpole relations. An interesting aspect of the analysis of the weak coupling limit is that the Calabi-Yau condition does not play any special role, nor the dimension of the base of the elliptic fibration. Moreover, topological relations like the F-theory-type-IIB D3 tadpole matching conditions are much more general than what we can expect from its F-theory origin. Indeed, the relation obtained for Euler characteristics can be lifted to a relation valid at the level of Chern classes. For an elliptic fibration $\varphi : Y \rightarrow B$ and a double cover of the base $\rho : X \rightarrow B$, we have

$$2\varphi_*c(Y) = 4\rho_*c(O) + \sum_j \rho_*c(D_j),$$

In this relation, the push-forwards bring the classes to the homology of B . This relation was already proven for Sen's weak coupling limit in [24]. In the case D_i is a Whitney umbrella, $\rho_*c(D_i)$ is understood as the Chern class of the normalization of D corrected by the Chern class of the pinch locus properly pushed-forward to the homology of B .

The more refined relations involving Chern classes are actually easier to prove than the relations at the level of the Euler characteristic, which end up being direct consequences of the Chern classes relations. In this context the Sethi-Vafa-Witten relation that gives the Euler characteristic of the elliptic fibration in terms of the intersection theory of the base follows from a simple Chern class relation. For an elliptic fibration $\varphi : Y \rightarrow B$ we get

$$\varphi_*c(Y) = (a + 1)c(Z),$$

where Z is a divisor of a suitable class, closely related to the fibration, and a is the number of distinguished sections of the fibration (see Remark 4.4). This formula is proved in Theorem 4.3 for E_8 , E_7 and E_6 elliptic fibrations, for which we have respectively $a = 1, 2, 3$. The Sethi-Vafa-Witten relation of the Euler characteristic is retrieved by simply evaluating the top Chern class of the previous equation.

1.7. E_8, E_7, E_6 families of elliptic fibrations. To be specific, we will study in this paper the weak coupling limits of E_8 , E_7 and E_6 elliptic fibrations. Each of these three families can be defined over an arbitrary smooth base B endowed with a line bundle \mathcal{L} . These are the most common families studied in the literature and generalize the traditional Legendre, Jacobi and Hesse family of elliptic fibrations. A large class of such Calabi-Yau fourfolds was obtained and their topological numbers computed in [35] in the context of Calabi-Yau hypersurfaces of weighted projective spaces. They also appear in the context of type IIB with Calabi-Yau three-folds [36, 37] and in F-theory with discrete torsion and reduced monodromy [38]. In our analysis, we do not restrict the dimension of the base nor do we impose the Calabi-Yau condition.

The E_8 elliptic fibration is the usual Weierstrass model written as a sextic in a weighted projective $\mathbb{P}_{1,2,3}^2$ bundle; the E_7 and E_6 fibrations are written respectively as a quartic in a $\mathbb{P}_{1,1,2}^2$ bundle and a cubic in a $\mathbb{P}_{1,1,1}^2$ bundle. They inherit their names from the theory of Del Pezzo surfaces [39]. In a strict sense, E_8 , resp. E_7 , E_6 singular fibers (types IV^* , resp. III^* , II^* in Kodaira's terminology) do not appear in the corresponding fibrations; they appear in specializations of these families, after a standard resolution process.

Remark 1.1. In this paper we are mostly interested in studying the actual fibers of the maps realizing our fibrations, before any resolution process: indeed, most of the families we consider will have a smooth total space, and in any case we find that the strict notion of

fiber that we use suffices for our general strategy producing weak coupling limits. See §2, and in particular Tables 2 and 3, for a list of the singular fibers that do appear in the main fibrations studied here.

Families of elliptic curves have been studied since at least as far back as the 18th century. Among the most famous ones we have the Legendre, Jacobi and Hesse families. They admit the following affine defining equations (see chapter 4 of [40]):

$$\begin{aligned} \text{Legendre family :} & \quad y^2 - x(x-1)(x-\lambda) = 0, \\ \text{Jacobi family :} & \quad y^2 - x^4 - 2\kappa x^2 - 1 = 0, \\ \text{Hesse family :} & \quad y^3 + x^3 + 1 - 3\mu xy = 0. \end{aligned}$$

These three families are toy models for the elliptic fibrations we will consider in this paper. They easily illustrate the fact that elliptic fibrations can have very different singular fibers. The Legendre family admits two singular fibers, one at $\lambda = 0$ and another at $\lambda = 1$. They are both nodal curves. The Jacobi family admits two singular fibers at $\kappa = \pm 1$, each corresponding to the union of two conics intersecting transversally at two different points. Finally, the Hesse family has one singular fiber at $\mu = 1$ and corresponding to 3 lines intersecting each other at one point and forming a triangle.

The study of E_8 , E_7 and E_6 Del Pezzo surfaces shows that they admit elliptic fibrations with fibers of type [39, 35]:

$$\begin{aligned} E_8 \text{ fiber :} & \quad y^2 + x^3 + z^6 + \lambda xyz = 0, \\ E_7 \text{ fiber :} & \quad y^2 + x^4 + z^4 - 2\kappa xyz = 0, \\ E_6 \text{ fiber :} & \quad y^3 + x^3 + z^3 - 3\mu xyz = 0. \end{aligned}$$

The previous equations are respectively written as a sextic in $\mathbb{P}_{1,2,3}^2$, a quartic in $\mathbb{P}_{1,1,2}^2$ and a cubic in $\mathbb{P}_{1,1,1}^2$ where the indices refer to the weights of $[z, x, y]$.

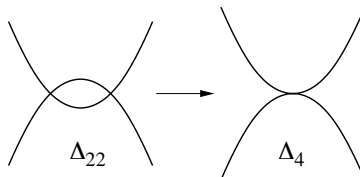
More generally, for us an E_8 , E_7 , or E_6 elliptic fibration is a smooth elliptic fibration written respectively as a sextic in a $\mathbb{P}_{1,2,3}^2$ -bundle, a quartic in a $\mathbb{P}_{1,1,2}^2$ -bundle, or a cubic in a $\mathbb{P}_{1,1,1}^2$ -bundle, and starting respectively as $y^2 + x^3$, $y^2 - x^4$, $y^3 + x^3$. They can always be put in the form:

$$\begin{aligned} E_8 \text{ fibration :} & \quad y^2 + x^3 + fxz^4 + gz^6 = 0, \\ E_7 \text{ fibration :} & \quad y^2 - x^4 - ex^2z^2 - fxz^3 - gz^4 = 0, \\ E_6 \text{ fibration :} & \quad y^3 + x^3 - dxyz - exz^2 - fyz^2 - gz^3 = 0, \end{aligned}$$

where in each cases, in order to balance the equation, the coefficients are sections of appropriate power of the line bundle \mathcal{L} over the base B . We will formalize this more carefully in §2. The Legendre, Jacobi and Hesse families are respectively specializations of the E_8 , E_7 and E_6 elliptic fibrations.

1.8. Examples of new weak coupling limits. We will present here some interesting configurations that would be non-generic and not supersymmetric in the usual Sen's limit with a smooth Weierstrass model, but which occur naturally in E_7 and E_6 fibrations.

1.8.1. *A supersymmetric brane-image-brane configuration.* In the E_7 case, we have 4 types of singular fibers. In view of the defining equation of an E_7 fibration, it is easy to see that the singular fibers correspond to choices of e, f, g such that the quartic polynomial $Q(x) = x^4 + ex^2z^2 + fxz^3 + gz^4$ admits multiple roots. All cases can be expressed in terms of partitions of 4. We will see in §2 that there are in total 4 types of singular fibers among which two are semistable (an ordinary nodal curve (Δ_{112}), and the transverse intersection of two conics (Δ_{22})) and two are unstable (a cusp (Δ_{13}) and two conics tangent at a point (Δ_4)). We define a weak coupling limit by a transition $\Delta_{22} \rightarrow \Delta_4$:



Δ_{22} is given by $f = 0, e^2 = 4g$ and $g \neq 0$ whereas Δ_4 is defined by $e = f = g = 0$. We get the following limit

$$\begin{cases} e = -2h \\ f = C\phi \\ g = h^2 + C\gamma \end{cases}$$

We see indeed that at $C = 0$ we are on Δ_{22} and when we specialize to $C = h = 0$ we are on Δ_4 . We have at leading order in C :

$$\Delta \sim C^2 h^2 (\gamma^2 - \phi^2 h), \quad j \sim \frac{1}{C^2} \frac{h^4}{\gamma^2 - \phi^2 h}.$$

Clearly when C goes to zero away from $h \neq 0$ we are at the weak coupling limit $j = \infty$. But when we specialize to $C = h = 0$, we get an undetermination $j = \frac{0}{0}$.

The interpretation of this D-brane configuration is as follows. In the base, we have the orientifold plane $\underline{O} : h = 0$ and a D7 brane-image-brane $\underline{D} : \gamma^2 - \phi^2 h = 0$. In order to appreciate that \underline{D} corresponds indeed to a brane-image-brane as seen in the base, we can move to the double cover $X : \xi^2 = h$, where the brane-image-brane will split into two components. We get the following brane spectrum:

$$O : \xi = 0, \quad D = D_+ + D_-, \quad D_{\pm} : \gamma \pm \phi\xi = 0.$$

We see that all the loci appearing here are smooth. The F-theory type IIB tadpole matching without flux gives

$$2\chi(Y) = 4\chi(O) + \chi(D_+) + \chi(D_-).$$

Since D_+ and D_- are isomorphic, they have the same Euler characteristic and therefore the tadpole matching relation simplifies to

$$\chi(Y) = 2\chi(O) + \chi(D_+).$$

Using the Sethi-Vafa-Witten relation for an E_7 fibration and the adjunction formula to compute the Euler characteristic of O and D_+ , it is easy to show that the tadpole matching relation holds without any need for fluxes (cf. §4.3.3). Therefore the brane-image-brane configuration does not break supersymmetry in contrast to the special configuration of a brane-image-brane in a Weierstrass model (see §4.4 of [25]).

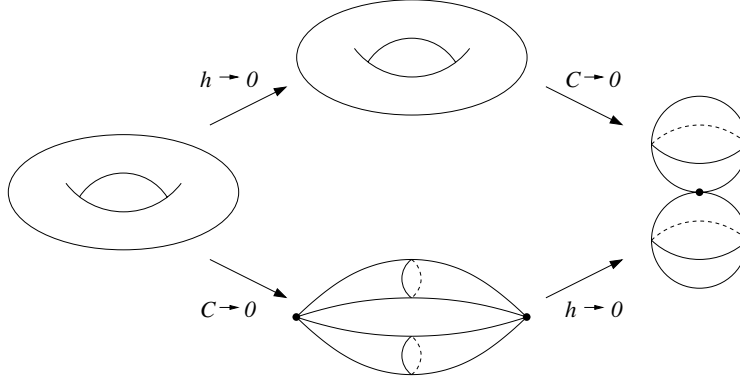
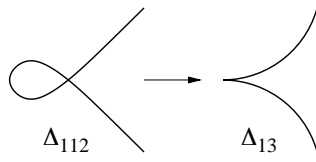


FIGURE 1. **Degeneration of the elliptic fiber as we take the weak coupling limit $C \rightarrow 0$.** This illustrates the case of the limit presented in §1.8.1 and §1.8.3. The limit $h \rightarrow 0$ is a specialization to the orientifold locus $h = 0$. As we take the weak coupling limit ($C \rightarrow 0$), the elliptic curve reduces to the union of two nonsingular rational curves intersecting transversally at two distinct points. Topologically, this is two spheres meeting at two distinct points. If we specialize to $h = 0$ as we take $C \rightarrow 0$, the two rational curves become tangent to each other at a point. In order to have a better understanding of the orientifold configuration, we can get to $C = h = 0$ by taking a different road. If we first specialize to $h = 0$ before taking the weak coupling limit, the elliptic fiber does not denegerate. However, once we take the weak coupling limit $C \rightarrow 0$ after taking $h = 0$, all the elliptic fibers flow to $e = f = g = 0$ which corresponds to two 2-spheres tangent at a point.

This tadpole relation holds at the level of Chern classes and for any dimension of the base and without the Calabi-Yau condition:

$$\varphi_*c(Y) = 2\rho_*c(O) + \rho_*c(D_+).$$

1.8.2. *A supersymmetric $D7$ Whitney - $D7$ -brane-image-brane configuration.* We can consider another limit defined by a transition $\Delta_{112} \rightarrow \Delta_{13}$. The details can be seen in §4.3.2:



The weak coupling limit is

$$\begin{cases} e = -6k^2 + h \\ f = -2k(4k^2 - h) + 2C\phi \\ f = -k^2(3k^2 - h) + 2Ck\phi + C^2\gamma \end{cases}$$

We get at leading order in C

$$\Delta \sim C^2 h^2 (h - 4k^2) (\phi^2 - h\gamma), \quad j \sim \frac{1}{C^2} \frac{h^4}{(h - 4k^2) (\phi^2 - h\gamma)}.$$

The D-brane spectrum is given by an orientifold plane $O : h = 0$, a D7 brane-image-brane $\underline{D}_1 : h - 4k^2$ and a singular D7 brane $\underline{D}_2 : \phi^2 - h\gamma$. As we move to the double cover $X : \xi^2 = h$, we get

$$O : \xi = 0, \quad D_{1\pm} : \xi \pm 2k = 0, \quad D_2 : \phi^2 - \xi^2\gamma = 0.$$

We see that O and $D_{1\pm}$ are all smooth whereas D_2 has the same singularities as in Sen's limit of a Weierstrass model. The D7-brane D_{1+} and its orientifold image are in the same class as O . Moreover, when k vanishes, the brane-image-brane D_{\pm} is on top of the orientifold plane and $j \sim h^3$: $D_{1+} = D_{1-} = O$ as $k \rightarrow 0$.

The F-theory/Type IIB tadpole matching relation gives

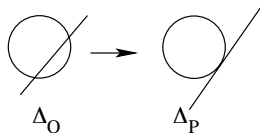
$$2\chi(Y) = 4\chi(O) + \chi(D_{1+}) + \chi(D_{1-}) + \chi_o(D_2).$$

We can simplify this relation by using $\chi(O) = \chi(D_{1+}) = \chi(D_{1-})$:

$$2\chi(Y) = 6\chi(O) + \chi_o(D_2).$$

This relation does hold. So we do not need fluxes here, and hence the brane-image-brane configuration does not break supersymmetry. In the F-IIB tadpole matching relation, we have used the Euler characteristic χ_o for D_2 since it has the singularities of a Whitney umbrella. The fact that the relation holds (verified in §4.3.2) is an additional non-trivial confirmation that this is the right Euler characteristic to use in orientifold theories.

1.8.3. *Two D7 brane-image-brane pairs in E_6 .* An E_6 fibration admits a rich list of possible transitions from semistable to unstable singular fibers. Here, we consider the specialization $\Delta_Q \rightarrow \Delta_P$ (with notation as in §2.2):



The semistable fiber Δ_Q is a specialization of a nodal curve. It corresponds to the transversal intersection of a conic with a line. The unstable curve Δ_P is a specialization of Δ_Q where the line and the conic become tangent to each other. The construction of this limit is given in details in section §3.4. The final result reads:

$$\begin{cases} d = 6k \\ e = 9k^2 + 3h \\ f = 9k^2 + 3h + C\phi \\ g = 2k(5k^2 + 3h) + C(\gamma + k\phi) \end{cases}.$$

At leading order in C , we have

$$j \sim \frac{1}{C^2} \cdot \frac{h^4}{(h + 3k^2)(\gamma^2 - h\phi^2)}.$$

We clearly reach the weak coupling limit when C goes to zero. The limiting discriminant is given by

$$\Delta_h = h^2(h + 3k^2)(\gamma^2 - h\phi^2).$$

Once we move to the double cover $X : \xi^2 = h$, this corresponds to an orientifold plane on $\xi = 0$. A D7 brane-image-brane on $D_{1\pm} : \gamma \pm \xi\phi = 0$ and another one on $D_{2\pm} : \xi \pm i\sqrt{3}k = 0$.

All these branes are wrapping smooth divisors. The brane-image-branes do not break supersymmetry since we can satisfy the F-theory-type-IIB tadpole relation without any need for fluxes:

$$2\chi(Y) = 4\chi(O) + \chi(D_{1+}) + \chi(D_{1-}) + \chi(D_{2+}) + \chi(D_{2-}).$$

Since $[D_{1+}] = [D_{1-}]$ and $[D_{2+}] = [D_{2-}] = [O]$, we obtain the simplified relation

$$\chi(Y) = 3\chi(O) + \chi(D_{1+}),$$

verified in §4.3.4.

1.9. Singularities and the weak coupling limit of F-theory. In the original E_8 limit considered by Sen, there is generally a unique D7 brane, wrapping a singular divisor with the singularities of a Whitney umbrella. We have presented here two E_7 limits, one admitting solely smooth divisors and another mixing smooth divisors and divisors with Whitney umbrella singularities, and one E_6 limit consisting of smooth divisors. It is natural to ask for a classification of all configurations of smooth divisors that can appear generally for E_8 , E_7 , and E_6 fibrations. The natural constraint to consider is that the configuration should satisfy the F-theory-type-IIB tadpole matching condition: this would ensure that it can be supersymmetric even in the presence of brane-image-brane pairs.

Surprisingly, this question has a very clean answer. Configurations satisfying the tadpole matching condition on unrestricted bases form an extremely short list: there are only three configurations of smooth divisors satisfying this constraint (Theorem 4.9). Two of these are precisely the E_7 and E_6 configuration we have realized by weak coupling limits; the third one is not realized as such, and cannot be realized in E_6 , E_7 , or E_8 fibrations. In particular, there are no configurations of smooth divisors satisfying the tadpole matching conditions in E_8 fibrations. This indicates that the appearance of the singular brane in Sen's limit cannot be avoided.

There are three additional configurations of smooth divisors satisfying the weaker requirement imposed by the tadpole matching condition in the Calabi-Yau case, for a base of dimension 3: one in E_8 , one in E_7 and one in E_6 . However, these extra three configurations have not yet been realized through weak coupling limits. See §4.4 for details.

2. FAMILIES OF ELLIPTIC FIBRATIONS AND THEIR SINGULAR FIBERS

In this section, we define the elliptic fibrations of type E_8 , E_7 and E_6 and study systematically their singular fibers (see Remark 1.1). We also introduce the notion of semistable and unstable fibers that will play a crucial role in explaining the geometric interpretation of the weak coupling limit.

We adopt the following terminology, after [35]. Let B be a nonsingular compact complex variety, endowed with a line bundle \mathcal{L} . We let $\mathcal{E} = \mathcal{O} \oplus \mathcal{L}_1 \oplus \mathcal{L}_2$, with $\mathcal{L}_1 = \mathcal{L}_2 = \mathcal{L}$, and we consider the projectivization $\mathbb{P}(\mathcal{E})$, with tautological line bundle $\mathcal{O}(1)$. An E_6 *elliptic fibration* over B is a nonsingular hypersurface Y of $\mathbb{P}(\mathcal{E})$, with equation

$$(1) \quad x^3 + y^3 = dxyz + exz^2 + fyz^2 + gz^3 \quad .$$

Here, z , x , and y are sections of $\mathcal{O}(1)$, $\mathcal{O}(1) \otimes \mathcal{L}$, and $\mathcal{O}(1) \otimes \mathcal{L}$, respectively, whose vanishing gives equations for the embeddings $\mathbb{P}(\mathcal{L}_1 \oplus \mathcal{L}_2) \subseteq \mathbb{P}(\mathcal{E})$, $\mathbb{P}(\mathcal{O} \oplus \mathcal{L}_2) \subseteq \mathbb{P}(\mathcal{E})$, $\mathbb{P}(\mathcal{O} \oplus \mathcal{L}_1) \subseteq \mathbb{P}(\mathcal{E})$, respectively. Note that these three loci have no common intersection; over each $p \in B$, the sections x , y , z serve as projective coordinates in the fiber of $\mathbb{P}(\mathcal{E})$

over p . The powers of \mathcal{L} appearing in \mathcal{E} are chosen so that (1) is balanced; the same requirement then determines the weights of d, e, f, g , so that the terms in (1) are sections of various line bundles as follows:

$$\begin{array}{c|c} z & \mathcal{O}(1) \\ \hline x & \mathcal{O}(1) \otimes \mathcal{L} \\ \hline y & \mathcal{O}(1) \otimes \mathcal{L} \end{array} , \quad \begin{array}{c|c} d & \mathcal{L} \\ \hline e, f & \mathcal{L}^2 \\ \hline g & \mathcal{L}^3 \end{array} .$$

With these positions, Y is the zero-set of a section of $\mathcal{O}(3) \otimes \mathcal{L}^3$ in $\mathbb{P}(\mathcal{E})$. The bundle projection induces a map $\varphi : Y \rightarrow B$; for every $p \in B$, the fiber $\varphi^{-1}(p)$ is the cubic curve in the fiber \mathbb{P}^2 of $\mathbb{P}(\mathcal{E})$ over p , defined by the equation (1) in the coordinates x, y, z . The nonsingularity of Y is guaranteed if the sections d, e, f, g are sufficiently general.

Similarly, an E_7 elliptic fibration over B is a nonsingular hypersurface Y with equation

$$(2) \quad y^2 = x^4 + ex^2z^2 + fxz^3 + gz^4$$

in a bundle of weighted projective planes $\mathbb{P}_{112}(\mathcal{O} \oplus \mathcal{L} \oplus \mathcal{L}^2)$ over B . Here, the terms appearing in (2) are sections of bundles as follows;

$$\begin{array}{c|c} z & \mathcal{O}(1) \\ \hline x & \mathcal{O}(1) \otimes \mathcal{L} \\ \hline y & \mathcal{O}(2) \otimes \mathcal{L}^2 \end{array} , \quad \begin{array}{c|c} e & \mathcal{L}^2 \\ \hline f & \mathcal{L}^3 \\ \hline g & \mathcal{L}^4 \end{array} .$$

We note that while $\mathcal{O}(2)$ is a line bundle on $\mathbb{P}_{112}(\mathcal{O} \oplus \mathcal{L} \oplus \mathcal{L}^2)$ (it is the restriction of the tautological line bundle via the natural embedding into $\mathbb{P}(\mathcal{O} \oplus \mathcal{L} \oplus \mathcal{L}^2 \oplus \mathcal{L}^2)$), $\mathcal{O}(1)$ only exists as a formal square root of $\mathcal{O}(2)$, due to the singularities of the weighted projective plane \mathbb{P}_{112} . However, Y is disjoint from these singularities, so this plays no role in our analysis of the geometry of Y , or in intersection-theoretic computations.

The hypothesis of nonsingularity implies that general fibers of E_6 or E_7 fibrations, given by equations of type (1), (2), resp. in \mathbb{P}^2 , \mathbb{P}_{112} , resp., are elliptic curves. The subtleties of the geometry of these fibrations is encoded in the *singular* fibers, whose type differs in the two types of fibrations.

E_8 fibrations may also be defined similarly, by an equation

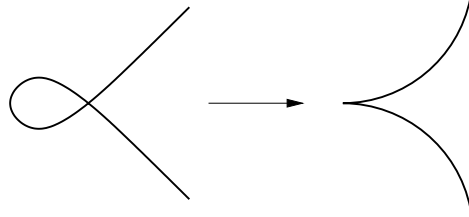
$$(3) \quad y^2 = x^3 + fxz^4 + gz^6$$

in a bundle of weighted projective planes $\mathbb{P}_{123}(\mathcal{O} \oplus \mathcal{L}^2 \oplus \mathcal{L}^3) \rightarrow B$; x, y , etc. are sections of line bundles as follows:

$$\begin{array}{c|c} z & \mathcal{O}(1) \\ \hline x & \mathcal{O}(2) \otimes \mathcal{L}^2 \\ \hline y & \mathcal{O}(3) \otimes \mathcal{L}^3 \end{array} , \quad \begin{array}{c|c} f & \mathcal{L}^4 \\ \hline g & \mathcal{L}^6 \end{array} .$$

These fibrations are studied in [24]⁶. The E_8 case is general in the sense that every elliptic curve can be put in Weierstrass normal form; this can be used to reduce the equations (1), (2) to the standard E_8 type, and it is useful in computing e.g. the j function and the discriminant locus of a fibration. However, this operation affects the singular fibers: in the E_8 case, the singular fibers may only be nodal (one singular point, with two distinct tangent lines) or cuspidal (one singular point, a ‘double’ tangent line). See Figure 1 for representative pictures; the arrow denotes that nodal curves can specialize to cuspidal curves in families.

⁶In [24] we place these fibrations in an ordinary projective bundle $\mathbb{P}(\mathcal{O} \oplus \mathcal{L}^3 \oplus \mathcal{L}^2)$. This does not affect the geometry of the fibration.

FIGURE 2. Singularities of E_8 fibrations

The discriminant has equation $4f^3 + 27g^2$, and the cuspidal locus has equations $f = g = 0$. The study of the corresponding stratification of the discriminant is an ingredient in [24].

Fibrations of type E_6 and E_7 as defined above have a richer catalog of possible singular fibers, and this information is key to the weak coupling limits studied in this paper. In the rest of this section we classify singular fibers of E_6 and E_7 fibrations.

2.1. Singularities of E_7 fibrations. Fibers of E_7 fibrations are obtained by specializing (2), that is, as curves with equation

$$(4) \quad y^2 = x^4 + ex^2z^2 + fxz^3 + gz^4$$

for fixed e, f, g . The Weierstrass model for this curve is

$$(5) \quad y^2 + x^3 + Fx + G = y^2 + x^3 + \left(-4g - \frac{1}{3}e^2\right)x + \left(-f^2 + \frac{8}{3}eg - \frac{2}{27}e^3\right) = 0 \quad .$$

Singularities of (4) are determined by the common vanishing of the three partial derivatives in x, y, z ; it follows that they are necessarily contained in $y = 0$, and in fact they coincide with the multiple solutions of the restriction of the curve to the line $y = 0$, which has equation

$$(6) \quad x^4 - ex^2z^2 - fxz^3 - gz^4 = 0 \quad .$$

This is a binary quartic form, which in general vanishes at four distinct points in the projective line $\mathbb{P}^1_{(x:z)}$. It acquires multiplicities when its discriminant vanishes:

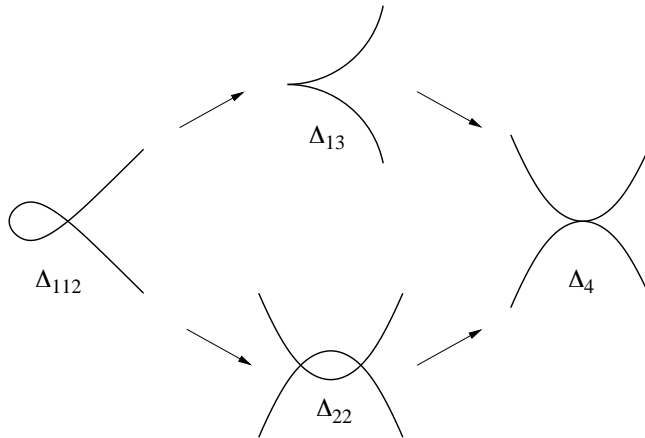
$$(7) \quad \Delta : \quad 4e^3f^2 + 27f^4 - 16e^4g + 128e^2g^2 - 144egf^2 - 256g^3 = 0 \quad .$$

This agrees with the discriminant $4F^3 + 27G^2 = 0$ of (5), and defines a hypersurface Δ of the base B .

To determine the different type of singular fibers, we note that the multiplicities of the zeros of a quartic form (6) can occur in one of 5 different ways, determined by the five partitions of the number 4. Thus there are four different types of forms (6) vanishing with multiplicities, and up to a change of the coordinates x, z they can be given as follows (listed together with the corresponding partitions):

$$\left\{ \begin{array}{ll} 1 + 1 + 2 & : \quad (x^2 - z^2)x^2 \\ 1 + 3 & : \quad (x + 3z)(x - z)^3 \\ 2 + 2 & : \quad (x^2 - z^2)^2 \\ 4 & : \quad x^4 \end{array} \right. \quad .$$

Since a linear change of coordinates does not affect the singularity type, this shows that there are four types of degenerate fibers in an E_7 elliptic fibration. Listed in terms of a representative equation, they are (cf. Figure 3):

FIGURE 3. Singularities of E_7 fibrations

- $y^2 = (x^2 - z^2)x^2$, a curve with a single singular point, a node;
- $y^2 = (x + 3z)(x - z)^3$, a curve with a single singular point, a cusp;
- $y^2 = (x^2 - z^2)^2$, the union of two nonsingular rational curves meeting transversally at two points;
- $y^2 = x^4$, the union of two nonsingular rational curves, meeting at one point and tangent to each other at that point.

These different types of singularities determine a stratification of the discriminant Δ into loci Δ_{112} , Δ_{13} , Δ_{22} , Δ_4 (indexed according to the corresponding partition), which is easy to determine explicitly. Indeed, it is easy to check that the quartic form (6) can be a fourth power only if $e = f = g = 0$:

$$(8) \quad \Delta_4 : \begin{cases} g = 0 \\ f = 0 \\ e = 0 \end{cases} ;$$

it is of type 2 + 2 if and only if it is

$$(9) \quad (x^2 - \alpha z^2)^2 = x^4 - 2\alpha x^2 z^2 + \alpha^2 z^4$$

for some $\alpha \neq 0$, that is:

$$\Delta_{22} : \begin{cases} g \neq 0 \\ f = 0 \\ e^2 = 4g \end{cases} ;$$

it is of type 3 + 1 if and only if it is

$$(x + 3\alpha z)(x - \alpha z)^3 = x^4 - 6\alpha^2 x^2 z^2 + 8\alpha^3 x z^3 - 3\alpha^4 z^4$$

for some $\alpha \neq 0$:

$$(10) \quad \Delta_{13} : \begin{cases} e \neq 0 \\ 8e^3 + 27f^2 = 0 \\ e^2 + 12g = 0 \end{cases} ;$$

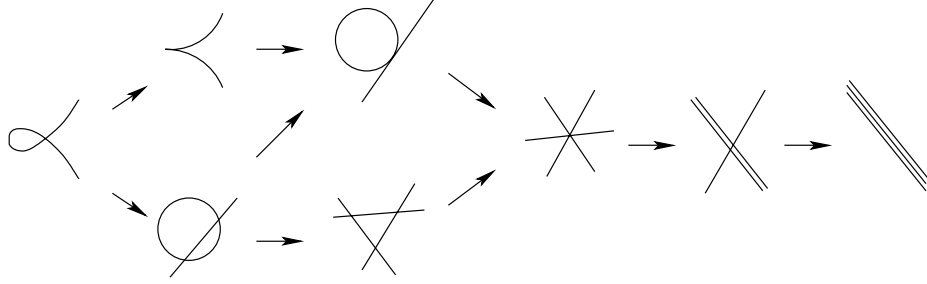


FIGURE 4. Singularities of cubic curves

and it is of type $1 + 1 + 2$ if it satisfies (7) but it does not satisfy any of the conditions listed above: $\Delta_{112} = \Delta \setminus (\Delta_{22} \cup \Delta_{13} \cup \Delta_4)$.

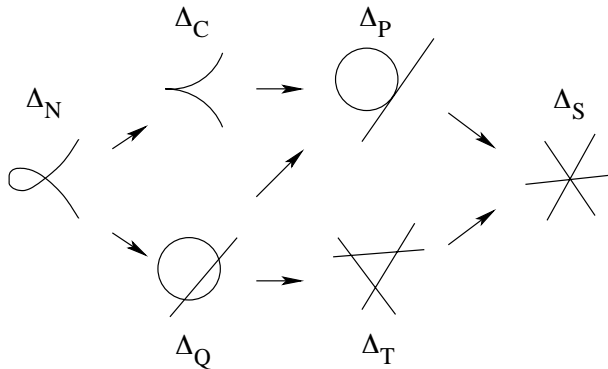
We can also note that Δ_{22} and Δ_{13} have codimension 1 in Δ , while Δ_4 has codimension 2. The intersection of the closures of Δ_{22} and Δ_{13} is Δ_4 ; this intersection is not transversal.

Finally, this stratification may be compared with the stratification of the discriminant of the Weierstrass model of the fibration. Stability considerations imply that the singular curves of the Weierstrass model will be cuspidal over Δ_4 and Δ_{13} , and nodal over Δ_{22} and Δ_{112} ; this can also be verified by an explicit computation.

2.2. Singularities of E_6 fibrations. The situation for E_6 fibrations is richer. In general, the possible singularities of a cubic plane curves are easily classified: an *irreducible* singular cubic is either nodal or cuspidal, and in fact isomorphic via a linear transformation to either $y^2z = x^3 + x^2z$ or $y^2z = x^3$; representative drawings for these two singularities are given in Figure 2. A *reducible* cubic must be the union of a nonsingular conic and a line, or of three lines, and it is easy to list the possible types of intersections and multiplicities that can occur. Figure 4 summarizes the situation, indicating specializations by arrows: for example, cubics decomposing as unions of a conic and a tangent line are in the closure of the set of cuspidal cubics, but ‘triangles’ are not.

We can use the following approach in classifying the singularities that can appear by specializing the equation (1) of an E_6 elliptic fibration: start from each type of singular cubic, and determine the relation on the coefficients d, e, f, g obtained by imposing that (1) is of the prescribed type. Qualitatively, the end-result of this analysis is represented graphically in Figure 5. The discriminant of (1) is stratified by loci $\Delta_N, \Delta_C, \Delta_Q, \Delta_P, \Delta_T, \Delta_S$. Each picture corresponds to a singular fiber, obtained over a point of the named locus; as above, arrows denote specialization. We also let $N = \overline{\Delta_N}, C = \overline{\Delta_C}$, etc.; thus, $\Delta_N = N \setminus (C \cup Q)$, etc. Equations for the six loci N, \dots, S in B will be given below. The codimension of N in B is 1; of C and Q , 2; of P and T , 3; and S has codimension 4; for example, $S = \emptyset$ if $\dim B = 3$ (and the sections are sufficiently general). The loci Q and P each consist of three components. The three components of Q meet precisely along the locus T . The three components of P likewise meet precisely along S .

A more thorough analysis suggests that (if the sections d, e, f, g are sufficiently general) the discriminant N is singular, with multiplicity 2 along C and Q , multiplicity 3 along P and T , and multiplicity 4 along S if $\dim B \geq 4$.

FIGURE 5. Singular fibers of E_6 fibrations

The Weierstrass form for (1) is

$$(11) \quad y^2 + x^3 + Fx + G$$

$$= y^2 + x^3 + \left(-3ef + \frac{9}{2}gd - \frac{1}{48}d^4\right)x + \left(-e^3 - f^3 + \frac{27}{4}g^2 + \frac{3}{4}efd^2 - \frac{5}{8}gd^3 - \frac{1}{864}d^6\right) = 0;$$

its discriminant is $4F^3 + 27G^2$, giving the equation of N :

$$N : 4 \left(-3ef + \frac{9}{2}gd - \frac{1}{48}d^4\right)^3 + 27 \left(-e^3 - f^3 + \frac{27}{4}g^2 + \frac{3}{4}efd^2 - \frac{5}{8}gd^3 - \frac{1}{864}d^6\right)^2 = 0$$

Over a general point of this hypersurface N , (1) defines an irreducible curve with a node; to verify this, it suffices to produce one such curve, and one may be obtained by setting $e = f = g = 0$, $d = 1$:

$$x^3 + y^3 = xyz$$

is an irreducible curve with a single node at $(z : x : y) = (1 : 0 : 0)$.

The j -invariant $\sim \frac{F^3}{4F^3 + 27G^2}$ of a cubic curve is defined (or ∞) if and only if the curve is not in the closure of the cuspidal locus; it follows that the the closure C of the locus parametrizing cuspidal curves has equations $F = G = 0$. Alternately, one can impose that the tangent cone at a singularity consists of a double line; this can be done by a Hessian computation, and leads to the equation $F = 0$; together with the discriminant $4F^3 + 27G^2$, this again shows that C has equations $F = G = 0$:

$$C : \begin{cases} -3ef + \frac{9}{2}gd - \frac{1}{48}d^4 = 0 \\ -e^3 - f^3 + \frac{27}{4}g^2 + \frac{3}{4}efd^2 - \frac{5}{8}gd^3 - \frac{1}{864}d^6 = 0 \end{cases}$$

To see that the general point of C indeed corresponds to an irreducible curve with an ordinary cusp, it suffices to produce one curve of this type and satisfying the equations for C ; one such curve is

$$x^3 + y^3 = 3xz^2 - 2z^3 \quad .$$

To proceed further, we describe explicitly the other singular curves represented in Figure 4, and find conditions on the coefficients d, e, f, g obtained by imposing that (1) matches the equations we obtain.

The general equation of the union of a line and a conic is:

$$(x + \rho y + \alpha z)(x^2 + \gamma xy + \delta y^2 + \epsilon xz + \phi yz + \beta z^2) = 0 \quad .$$

We may assume that the coefficients of x, x^2 in the two factors are 1, since the product will have to match (1). For the match to occur, it is necessary that the coefficients of x^2y, x^2z, xy^2, y^2z all vanish. The first two constraints give

$$\gamma = -\rho \quad , \quad \epsilon = -\alpha \quad ;$$

the third then forces

$$\delta = \rho^2 \quad ;$$

and the fourth translates into

$$\rho(\phi + \alpha\rho) = 0 \quad .$$

At this point the coefficient of y^3 is ρ^3 ; matching (1) forces $\rho^3 = 1$, and in particular $\rho \neq 0$, yielding

$$\phi = -\alpha\rho \quad .$$

The conclusion is that these curves are in the form represented by (1) if and only if they are in fact

$$(12) \quad (x + \rho y + \alpha z)(x^2 - \rho xy - \alpha xz + \rho^2 y^2 - \alpha \rho yz + \beta z^2) = 0 \quad ,$$

with ρ a cubic root of 1:

$$\rho = 1 \quad \text{or} \quad \frac{-1 \pm i\sqrt{3}}{2} \quad .$$

Expanding (12) and matching with (1) we find that

$$\begin{cases} d = 3\rho\alpha \\ e = \alpha^2 - \beta \\ f = \rho(\alpha^2 - \beta) \\ g = -\alpha\beta \end{cases} \quad ,$$

and eliminating α, β (ρ is already determined up to a finite choice) gives the equations

$$(13) \quad \boxed{Q : \begin{cases} f = \rho e \\ g = \frac{d(9\rho^2 e - d^2)}{27} \end{cases} \quad , \quad \rho^3 = 1 \quad .}$$

The three allowed values for ρ give three (clearly irreducible) components of the locus Q over which the fibers of (1) consist of the union of a line and a conic. For example, taking $\rho = 1$ and $e = f = -1, d = g = 0$, gives

$$x^3 + y^3 + xz^2 + yz^2 = (x + y)(x^2 - xy + y^2 - z^2) = 0 \quad ,$$

the union of a line and a nonsingular conic meeting transversally. Similar examples may be given on the other two components, showing that the general fiber over each of the three components is of the same type.

Also note that from the above discussion it follows that, on Q , we must have

$$\alpha = \frac{\rho^2 d}{3}, \quad \beta = \frac{\rho d^2}{9} - e, \quad \gamma = -\rho, \quad \delta = \rho^2, \quad \epsilon = -\frac{\rho^2 d}{3}, \quad \phi = -\frac{d}{3}, \quad (\rho^3 = 1).$$

The fiber over a general point of Q consists of the union of the line $x = -\rho y - \alpha z$ and the conic $x^2 - \rho xy - \alpha xz + \rho^2 y^2 - \alpha \rho yz + \beta z^2 = 0$; intersecting these two components gives the polynomial in x, z :

$$3\rho^2 y^2 + 3\alpha \rho yz + (2\alpha^2 + \beta)z^2 \quad ;$$

the line intersect the conic in a double point if this polynomial has a double root, that is, when its discriminant vanishes. This is true if and only if

$$5\alpha^2 + 4\beta = 0 \quad .$$

As shown above, on Q this is equivalent to

$$5\left(\frac{\rho^2 d}{3}\right)^2 + 4\left(\frac{\rho d^2}{9} - e\right) = 0 \quad ,$$

that is,

$$4e = \rho d^2 \quad .$$

Putting this equation together with the equations for Q gives equations for P :

$$(14) \quad \boxed{P : \begin{cases} f = \rho e = \frac{\rho^2 d^2}{4} \\ g = \frac{5d^3}{108} \end{cases}, \quad \rho^3 = 1}$$

It is easy to check that $P = C \cap Q$; this is not a transversal intersection. A typical point of P may be obtained by setting $\rho = 1$ and $d = -6$; solving for e, f, g gives the curve

$$x^3 + y^3 + 6xyz - 9xz^2 - 9yz^2 + 10z^3 = (x + y - 2z)(x^2 - xy + 2xz + y^2 + 2yz - 5z^2) = 0$$

It is easy to check that the conic is nonsingular, and the line is tangent to it at the point $(z : x : y) = (1 : 1 : 1)$.

The other way in which a curve consisting of a line union a transversal conic may degenerate is as a triangle of nonconcurrent lines; this happens precisely when the conic becomes singular. The conic has equation

$$x^2 - \rho xy - \alpha xz + \rho^2 y^2 - \alpha \rho yz + \beta z^2 = 0 \quad ,$$

and imposing that the three partials have a common root gives the condition $\beta = \alpha^2$. As seen above, on Q this is equivalent to $e = 0$. Putting together with the equations for Q gives the equations for the locus T parametrizing triangles:

$$\boxed{T : \begin{cases} e = f = 0 \\ g = -\frac{d^3}{27} \end{cases}} \quad .$$

A typical fiber over a point of T is obtained by taking $d = 3$, which gives

$$x^3 + y^3 + z^3 = 3xyz \quad .$$

This factors (over \mathbb{C}) as a product of three nonconcurrent lines.

The triangle may degenerate by having the vertices come together. The resulting locus S of ‘stars’ may be viewed as the intersection of P and T , and hence has equations

$$\boxed{S : \quad d = e = f = g = 0} \quad .$$

FIGURE 6. Unstable fibers of E_8 , E_7 , E_6 fibrationsFIGURE 7. Semistable fibers of E_8 , E_7 , E_6 fibrations

In other words, the only singular fiber of this type is the curve

$$x^3 + y^3 = 0 \quad .$$

Since the star is isolated, the fibers cannot degenerate further. Thus, the last two (nonreduced) types of singular cubics shown in Figure 4 cannot occur in the family given by (1). This completes the classification of singular fibers in a fibration with equation (1).

Finally, one can examine the behavior of fibers of the corresponding Weierstrass model over the strata of the discriminant. Since F and G vanish along C , these fibers are cuspidal curves over Δ_C and its specializations Δ_P and Δ_S . Since $F \neq 0$ along the other loci, the fibers of the Weierstrass model are nodal over Δ_N , Δ_Q , and Δ_T .

2.3. Semistable and unstable fibers. In each of the cases considered in this section, we will refer to the fibers over the closure of the cuspidal loci as *unstable*, and to the other types as *semistable*; see Figures 6 and 7.

This terminology is borrowed from algebraic geometry. The distinguishing features of the curves in Figure 6 is that the j invariant is *not* defined for these curves. These are the curves for which the coefficient F in the corresponding Weierstrass model vanishes; since the discriminant $\Delta = 4F^3 + 27G^2$ vanishes for all singular curves, the quotient F^3/Δ (which equals j , up to a multiple) is undefined for unstable curves. By contrast, $F \neq 0$ for semistable curves; their j invariant is unambiguously defined to be ∞ .

This distinction will be useful in §3.

3. WEAK COUPLING LIMITS

The analysis carried out in §2 provides us with a key element of information in the construction of ‘weak coupling limits’ in the style of Sen’s celebrated work ([23]). Our strategy is to focus on the specialization of a type of singular fiber to another in the situations encountered in §2, in a way that we describe in general terms in §3.2. We precede this description with a revisit of Sen’s E_8 limit, in §3.1; we follow it in §3.3 and §3.4 with applications of the strategy to the E_7 and E_6 environments, obtaining new weak coupling limits.

In §3.5 we clarify the reasons underlying the choices inherent to our procedure.

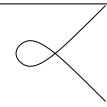
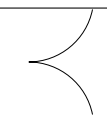
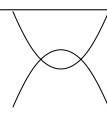
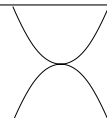
Name	Conditions	Type of singular fiber (Kodaira notation)	
Δ_{112}	$g \neq 0, \quad f = 0, \quad e^2 = 4g$	I_1	
Δ_{13}	$e \neq 0, \quad 8e^3 + 27f^2 = 0, \quad e^2 + 12g = 0$	II	
Δ_{22}	$g \neq 0, \quad f = 0, \quad e^2 = 4g$	I_2	
Δ_4	$e = f = g = 0$	III	

TABLE 2. Singular fibers of E_7 elliptic fibrations

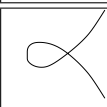

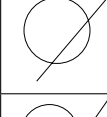
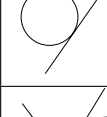
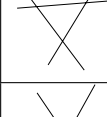
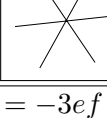
Name	Conditions	Type of singular fiber (Kodaira notation)	
Δ_N	$\Delta = 0$	I_1	
Δ_C	$F = G = 0$	II	
Δ_Q	$f = \rho e, \quad g = \frac{1}{27}d(9\rho^2 e - d^2)$	I_2	
Δ_P	$f = \rho e, \quad e = \frac{1}{4}\rho d^2, \quad g = \frac{5}{108}d^3$	III	
Δ_T	$e = f = 0, \quad g = -\frac{1}{27}d^3$	I_3	
Δ_S	$d = e = f = g = 0$	IV	

TABLE 3. Singular fibers of E_6 elliptic fibrations. Here $\rho^3 = 1$, $F = -3ef + \frac{9}{2}gd - \frac{1}{48}d^4$, $G = -e^3 - f^3 + \frac{27}{4}g^2 + \frac{3}{4}efd^2 - \frac{5}{8}gd^3 - \frac{1}{864}d^6$, and $\Delta = 4F^3 + 27G^2$.

3.1. Sen's limit, revisited. Here we review the limit for E_8 fibrations considered by Ashoke Sen in [23], in a way which emphasizes the general features of the strategy we will apply to E_7 and E_6 in the rest of the section.

As recalled in §2, E_8 fibrations may be defined by equation (3):

$$y^2 = x^3 + f x z^4 + g z^6$$

in a bundle of weighted projective planes $\mathbb{P}_{123}(\mathcal{O} \oplus \mathcal{L}^2 \oplus \mathcal{L}^3) \rightarrow B$. Note that in the E_8 case we have only one type of semistable fiber and one type of unstable fiber: nodal and cuspidal curves, respectively. In terms of the parameters f and g , the fiber is a nodal curve when

$$(15) \quad 4f^3 + 27g^2 = 0 \quad , \quad f \neq 0$$

while the unstable locus is

$$f = g = 0 \quad .$$

We view this situation in a parameter space with coordinates f, g . In this space, (15) represents a cuspidal curve, which admits the standard parametrization

$$h \mapsto (f, g) = (-3h^2, -2h^3) \quad .$$

This motivates us to define a degenerate fibration Y_h by setting

$$(16) \quad \begin{cases} f = -3h^2 \\ g = -2h^3 \end{cases} \quad ,$$

or in divisor form

$$Y_h : \quad y^2 = x^3 - 3h^2 x z^4 - 2h^3 z^6 = (x + h z^2)^2 (x - 2h z^2) \quad .$$

Note that since f, g are resp. sections of $\mathcal{L}^4, \mathcal{L}^6$, this can be achieved with h a section of \mathcal{L}^2 ; this will be one of the requirements that we will pose in §3.2. Also note that $f = g = 0$ precisely if $h = 0$; thus, the fibers of Y_h over points of \underline{Q} (the hypersurface $h = 0$ in B) are unstable (i.e., cuspidal), and the fibers over points of $B \setminus \underline{Q}$ are semistable (i.e., nodal); this will also be a general feature of our construction.

Next, we perturb Y_h to get a general family $Y_h(C)$. We perturb the assignment for f in (16) with a general choice of a section η :

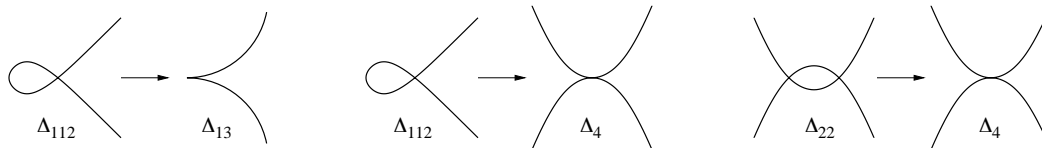
$$f = -3h^2 + C\eta \quad ,$$

where η is a general section of \mathcal{L}^4 . Setting likewise $g = -2h^3 + C\gamma$, one sees that $j \propto h^3$ at leading order in C unless $\gamma = h\eta$. The case $j \propto h^3$ is interesting (see §1.2): it corresponds to a bound state of the orientifold with a brane-image-brane on top of it. We will consider the general case of $j \sim h^{4-n}$, $n = 0, 1, 2, 3, 4$ in §3.5. However, we will in general insist that $j \propto h^4$, corresponding to a pure O7-orientifold. This prompts us to set $g = -2h^3 + Ch\eta$ at first order in C , and adding a further term to achieve generality we arrive at the description of $Y_h(C)$:

$$\begin{cases} f = -3h^2 + C\eta \\ g = -2h^3 + Ch\eta + C^2\chi \end{cases} \quad ,$$

with h, η, χ resp. general sections of $\mathcal{L}^2, \mathcal{L}^4, \mathcal{L}^6$, resp. This is precisely the limit considered by Sen. With these positions,

$$j \sim \frac{1}{C^2} \cdot \frac{h^4}{\eta^2 + 12h\chi}$$

FIGURE 8. Allowed specializations for E_7 fibrations

at leading order in C . Studying the limiting discriminant $h^2(\eta^2 + 12h\chi)$ and its pull-back to the double cover X over B ramified along \underline{Q} leads to interesting Euler characteristics and Chern class identities, explored in [24].

3.2. The strategy. We now abstract the key points of the procedure leading to Sen's limit in §3.1. In order to produce weak coupling limits for the elliptic fibrations considered in §2 we propose the following procedure:

- choose a specialization of a semistable singular fiber S_1 to an unstable one S_2 among the types listed in §2;
- realize the specialization by means of a section h of \mathcal{L}^2 , producing a degenerate family Y_h for which the fiber over the hypersurface \underline{Q} defined by $h = 0$ is of type S_2 , and the general fiber (over $B \setminus \underline{Q}$) is of type S_1 ;
- perturb Y_h to a general family $Y_h(C)$ depending on a scalar parameter C , for which the j invariant behaves at leading order in C as

$$j \sim \frac{1}{C^r} \cdot \frac{h^4}{D}$$

for some $r > 0$. Here, \underline{D} will be a component (or a collection of components) of the limiting discriminant Δ_h of $Y_h(C)$ as $C \rightarrow 0$ (that is, the leading term of the discriminant $\Delta_h(C)$ of $Y_h(C)$). The other component of this limiting discriminant is supported on \underline{Q} .

For example, $j \sim h^4$ ensures the right charge for a pure O7-brane. In practice, satisfying the two basic requirements that h be a section of \mathcal{L}^2 and that $j \sim h^4$ usually leads to nontrivial constraints, and can be achieved only for certain choices of the specialization $S_1 \rightarrow S_2$. Whenever we are successful in carrying out this program, we can consider the double cover X of B ramified along \underline{Q} . The case of greatest physical interest is the case in which both X and Y are Calabi-Yau varieties, which corresponds to $c_1(\mathcal{L}) = c_1(TB)$. In this case we will identify the ramification locus O of $X \rightarrow B$ as the support of an orientifold, and the preimage D of \underline{D} in X as carrying D7 branes. Every such situation leads then to the prediction of a tadpole relation between the Euler characteristics of these loci. More details for these constructions are given in §4.

A few comments motivating more explicitly the specific requirements listed here will be given in §3.5.

3.3. Two E_7 weak coupling limits. We now apply the strategy reviewed in §3.2 to E_7 elliptic fibrations, with equation (2):

$$y^2 = x^4 + ex^2z^2 + fxz^3 + gz^4 \quad .$$

The choice of a specialization from a semistable to an unstable fiber is restricted to the list given in Figure 8. We first choose to specialize $\Delta_{22} \rightarrow \Delta_4$. The closure of Δ_{22} has equations

(cf. (2.1)):

$$e^2 = 4g \quad , \quad f = 0 \quad .$$

Viewing e, f, g as coordinates in a parameter space, these equations describe a nonsingular conic curve, parametrized by

$$h \mapsto (e, f, g) = (-2h, 0, h^2) \quad .$$

This parametrization leads to the following description of the degenerate fibration Y_h :

$$(17) \quad \begin{cases} e = -2h \\ f = 0 \\ g = h^2 \end{cases} \quad ,$$

in divisor form

$$Y_h : \quad y^2 = x^4 - 2hx^2z^2 + h^2z^4 = (x^2 - hz^2)^2 \quad .$$

We note that this is done by choosing h to be a general section of \mathcal{L}^2 , thus satisfying one of the basic requirements from §3.2; and that $g = 0$ if and only if $h = 0$, so that the specialization Δ_4 is attained precisely over $h = 0$, also as prescribed in §3.2.

We next perturb (17) in the simplest way needed to produce a general family $Y_h(C)$:

$$\begin{cases} e = -2h \\ f = C\phi \\ g = h^2 + C\gamma \end{cases} \quad .$$

With this choice,

$$j \sim \frac{1}{C^2} \cdot \frac{h^4}{\gamma^2 - \phi^2 h}$$

at leading order: thus, all the requirements listed in §3.2 are satisfied. The limiting discriminant has equation

$$(18) \quad h^2 (\gamma^2 - \phi^2 h) = 0 \quad :$$

with notation as in §3.2, \underline{D} is the hypersurface $\gamma^2 - \phi^2 h = 0$. In the double cover $X : \xi^2 = h$, this hypersurface splits into two smooth components D_{\pm} that are mapped to each other by the orientifold involution, so that this hypersurface corresponds to a brane-image-brane pair. See §1.8.1 and §4.3.3 for a description of the corresponding configuration of O7 and D7 in the double cover, and for a precise identity of Euler characteristics related to this configuration.

A second possible choice of specialization is $\Delta_{112} \rightarrow \Delta_{13}$, leading to a different limit. We follow the same procedure: in the parameter space (e, f, g) , the closure of Δ_{13} is parametrized by

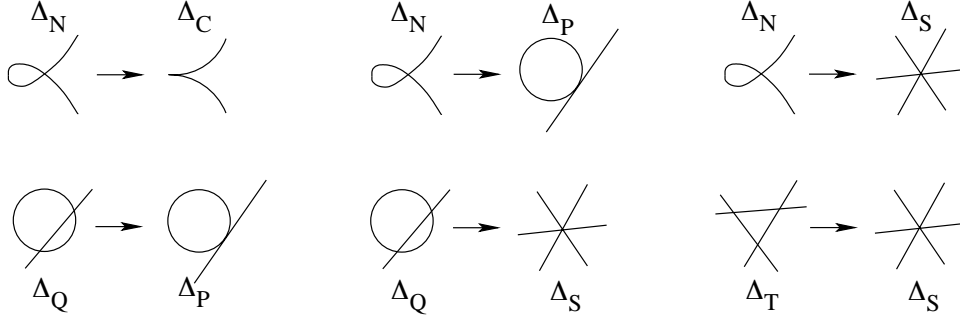
$$k \mapsto (e, f, g) = (-6k^2, -8k^3, -3k^4)$$

(see (10)). We can extend this to a parametrization of $\overline{\Delta_{112}}$:

$$(k, h) \mapsto (e, f, g) = (-6k^2 + h, -2k(4k^2 - h), -k^2(3k^2 - h))$$

yielding the degenerate fibration Y_h :

$$\begin{cases} e = -6k^2 + h \\ f = -2k(4k^2 - h) \\ g = -k^2(3k^2 - h) \end{cases} \quad .$$

FIGURE 9. Allowed specializations for E_6 fibrations

Here, k, h are general sections of $\mathcal{L}, \mathcal{L}^2$, respectively. The fiber is of type Δ_{112} over $B \setminus \underline{Q}$, and generally of type Δ_{13} over \underline{Q} , degenerating further to type Δ_4 over $h = k = 0$.

As in Sen's limit, perturbing Y_h in the simplest way by adding linear terms in C to f and g leads to a situation for which $j \propto h^3$, unless a simple constraint between these terms is satisfied. We satisfy this constraint and add a C^2 term to preserve generality, obtaining the following family $Y_h(C)$:

$$\begin{cases} e = -6k^2 + h \\ f = -2k(4k^2 - h) + 2C\phi \\ g = -k^2(3k^2 - h) + 2Ck\phi + C^2\gamma \end{cases} .$$

For this family,

$$j \sim \frac{1}{C^2} \cdot \frac{h^4}{(h - 4k^2)(\phi^2 - h\gamma)}$$

at leading order in C , with limiting discriminant

$$(19) \quad \Delta_h = h^2(h - 4k^2)(\phi^2 - h\gamma) .$$

The geometry of this situation has similarities with Sen's limit, and also leads to an Euler characteristic/Chern class identity, in which the singularities of the support of Δ_h play a key role; see §1.8.2 and §4.3.2. In the double cover $X : \xi^2 = h$, the brane spectrum will consist on an orientifold, a smooth brane-image-brane pair resulting from the splitting of $h - 4k^2$, and a singular 'Whitney brane' (see §1.1) corresponding to the component $(\phi^2 - h\gamma)$ of the discriminant. These singularities are typical of Sen's limit.

3.4. An E_6 weak coupling limit. The situation for E_6 fibrations is in principle richer. There are several allowed specializations, shown in Figure 9; we focus on the $\Delta_Q \rightarrow \Delta_P$ case. Recall that Q and P each consists of three components; according to (13) (choosing $\rho = 1$), equations for one component of Q are

$$(20) \quad f = e \quad , \quad g = \frac{d(9e - d^2)}{27}$$

and equations for the corresponding component of P are (from (14))

$$(21) \quad f = e = \frac{d^2}{4} \quad , \quad g = \frac{5d^3}{108} .$$

Again we take the parameters d, e, f, g of the fibrations as coordinates of a parameter space, and study the loci defined by (20) and (21) in this space. We note that (21) can be parametrized as follows:

$$k \mapsto (d, e, f, g) = (6k, 9k^2, 9k^2, 10k^2) \quad ;$$

and this is easily extended to a parametrization of (20):

$$(k, h) \mapsto (d, e, f, g) = (6k, 9k^2 + 3h, 9k^2 + 3h, 2k(5k^2 + 3h)) \quad .$$

Accordingly, we choose the degenerate fibration Y_h to be given by

$$(22) \quad \begin{cases} d = 6k \\ e = 9k^2 + 3h \\ f = 9k^2 + 3h \\ g = 2k(5k^2 + 3h) \end{cases} \quad .$$

Here, k is a general section of \mathcal{L} , and h is a general section of \mathcal{L}^2 ; once more, this fulfills one of the basic requirements of §3.2. The fibers over points on $\underline{Q} = \{h = 0\}$ are of the unstable type Δ_P (they degenerate further to type Δ_S where both h and k vanish); over $B \setminus \underline{Q}$, they are of type Δ_Q , as required.

Next, we perturb (22) in order to construct an associated general family $Y_h(C)$. Since d and e may already be assumed to be general (as k and h are general), we only need to perturb f and g :

$$\begin{cases} d = 6k \\ e = 9k^2 + 3h \\ f = 9k^2 + 3h + C\phi \\ g = 2k(5k^2 + 3h) + C\chi \end{cases} \quad .$$

With these positions, the discriminant $\Delta_h(C)$ is

$$\Delta_h(C) \sim C^2 h^2 (h + 3k^2) ((\chi - k\phi)^2 - h\phi^2)$$

at leading order in C . We set $\gamma = \chi - \phi k$, to simplify this expression (without affecting geometric properties of the family), and we obtain the following description for the general family $Y_h(C)$:

$$\begin{cases} d = 6k \\ e = 9k^2 + 3h \\ f = 9k^2 + 3h + C\phi \\ g = 2k(5k^2 + 3h) + C(\gamma + k\phi) \end{cases} \quad .$$

For this family,

$$j \sim \frac{1}{C^2} \cdot \frac{h^4}{(h + 3k^2)(\gamma^2 - h\phi^2)}$$

to leading order in C . Thus, all requirements set forth in §3.2 are satisfied, with limiting discriminant

$$(23) \quad \Delta_h = h^2 (h + 3k^2) (\gamma^2 - h\phi^2) \quad .$$

The D-brane spectrum was determined in §1.8.3 and consists of an orientifold and two brane-image-brane pairs; see §4.3.4 for a discussion of the tadpole relation for this limit.

3.5. Discussion. In this subsection we motivate the choices leading to the strategy explained in §3.2. These are principally the following:

- we specialize a *semistable* fiber S_1 to an *unstable* fiber S_2 ;
- the parameter h controlling the degenerate fibration Y_h is a section of \mathcal{L}^2 ; the fiber of this degenerate fibration is S_1 at all points of B where h does *not* vanish;
- $j \propto h^4$ at leading order in C , up to a factor depending on the other components of the limiting discriminant.

For $Y_h(C)$,

$$j \propto \frac{F^3}{4F^3 + 27G^2} \quad ,$$

where F and G are the parameters of the Weierstrass model of $Y_h(C)$; F is a section of \mathcal{L}^4 , and G is a section of \mathcal{L}^6 . The term of lowest order in C in the denominator defines the limiting discriminant, a section of \mathcal{L}^{12} . We factor it as $h^a \underline{D}$ for some $a \geq 0$ and a term \underline{D} which is not a multiple of h .

The fact that the general degenerate fiber S_1 is semistable guarantees that F is not a multiple of C , so that generally $j \rightarrow \infty$ as $C \rightarrow 0$:

$$j \sim \frac{1}{C^r} \cdot \frac{F^3|_{C=0}}{h^a \underline{D}}$$

at leading order in C , for some $r > 0$. Since the fiber of Y_h is semistable where $h \neq 0$, it follows that $F|_{C=0}$ divides a power of h , so in fact $F|_{C=0}$ equals a power of h up to a constant multiple.

In particular, a power of h is a section of \mathcal{L}^4 ; the most natural way to achieve this is by assuming that h is itself a section of \mathcal{L}^c for some $c|4$: $c = 1, 2$, or 4 . Now note that since C divides $4F^3 + 27G^2$, it follows that $G|_{C=0}$ is also a power of h , and by the same token we see that $c|6$. Thus necessarily $c = 1$ or 2 . As our basic geometric construction demands that we take a *double* cover of B ramified along the hypersurface \underline{Q} given by $h = 0$, it is natural to assume that $c = 2$: this justifies our requirement that h be a section of \mathcal{L}^2 . Thus

$$j \sim \frac{1}{C^r} \cdot \frac{h^6}{h^a \underline{D}} \quad .$$

Note that in particular $F|_{C=0} = 0$ over points of the hypersurface \underline{Q} defined by $h = 0$; thus, the special degenerate fiber S_2 is necessarily unstable, as we prescribe.

Finally, we take into account the D7 tadpole relation ((1) in §1.5): \underline{D} must be a section of \mathcal{L}^8 if O corresponds to a pure orientifold, and as $h^a \underline{D}$ is a section of \mathcal{L}^{12} and h is a section of \mathcal{L} , this forces $a = 2$. Thus $j \propto h^4$ in the pure orientifold case, and this justifies our last requirement.

It is in fact interesting to consider cases in which at $h = 0$ we have a bound state of one orientifold and n brane-image-branes: one example has already been illustrated in §1.2, and several will be listed in §5. In this case, \underline{D} is a multiple of h^n , and $j \sim h^{4-n}$. The case $n = 0$ gives $j \sim h^4$ and corresponds to a pure orientifold. The extreme case $n = 4$ corresponds to $\Delta \sim h^6$, giving 4 brane-image-branes on top of the orientifold. This can be obtained as specialization of several limits listed in §5.

4. TADPOLE RELATIONS

In this section we review intersection-theoretic aspects of the limits found in §3. As we will explain in §4.1, tadpole matching in type IIB and F-theory leads to identities relating the Euler characteristic of the total space Y of the fibration, and loci in the double cover X of B ramified along the hypersurface \underline{Q} with equation $h = 0$. These loci are the preimages in X of the components of the limiting discriminant Δ_h : the preimage O of \underline{Q} , where the orientifold is located, and the preimage D of the other components \underline{D} .

The identities predicted by the physics considerations of §4.1 hold when X and Y are Calabi-Yau varieties, of dimension 3 and 4, respectively. The results in this section will show that these predictions have a much broader range of validity: suitably interpreted, the identities will hold in arbitrary dimension, and for varieties that are not necessarily Calabi-Yau.

We note here that the Calabi-Yau case corresponds to the case in which the basic line bundle \mathcal{L} on B is the anticanonical line bundle. Here and in the following, we denote by $c_i(V)$ the i -th Chern class $c_i(TV)$ of the tangent bundle of the variety V .

Proposition 4.1. *With X and Y as above, and with notation as in §2 and §3, X and Y are both Calabi-Yau varieties if $c_1(\mathcal{L}) = c_1(B)$.*

In fact, Y is a Calabi-Yau if $c_1(\mathcal{L}) = c_1(B)$; X is a Calabi-Yau if $[Q] = 2c_1(B)$. Thus, in the Calabi-Yau case this gives a second motivating reason to require h to be a section of \mathcal{L}^2 , beside the more general considerations of §3.5.

The proof of Proposition 4.1 is standard [23], so we leave it to the reader⁷.

While the case $c_1(\mathcal{L}) = c_1(B)$ is therefore the most significant for physical applications, we stress that the identities we will study in this section will in fact hold without this additional hypothesis.

4.1. F-theory-type-IIB tadpole matching condition. F-theory is a strongly coupled version of type IIB string theory. It realizes geometrically the S -duality group of type IIB. One of the strongest constraints in compactified theory is the cancellation of the tadpole. This can be seen as a direct consequence of Gauss's law: the total charge in a compact space has to vanish since the flux has nowhere to go.

In the context of string theory with D-branes, the tadpole condition requires the vanishing of all D-brane charges. This is complicated by the fact that higher dimensional D-branes admit lower brane charges due to Chern-Simons terms included to cancel anomalies. In the context of type IIB with O3/O7 planes, this is especially important for D7 branes and O7 planes wrapping divisors of the Calabi-Yau three-fold. They have an induced D3 charge given by the Euler characteristic of the divisor they wrap. The D3 tadpole also has

⁷As an illustration, consider the E_6 case. Then Y is defined by a divisor of class $c_1(\mathcal{O}(3) \otimes \mathcal{L}^3)$ in the projectivization $\pi : \mathbb{P}(\mathcal{E}) \rightarrow B$, where $\mathcal{E} = \mathcal{O} \oplus \mathcal{L} \oplus \mathcal{L}$. By e.g., B.5.8 in [41],

$$c_1(\mathbb{P}(\mathcal{E})) = \pi^* c_1(B) + \pi^* c_1(\mathcal{E}) + 3c_1(\mathcal{O}(1)) = \pi^* c_1(B) + 2\pi^* c_1(\mathcal{L}) + 3c_1(\mathcal{O}(1)) \quad ;$$

by the adjunction formula, therefore,

$$c_1(Y) = (\varphi^* c_1(B) + \varphi^* c_1(\mathcal{E}) + 3c_1(\mathcal{O}(1))) - (3c_1(\mathcal{L}) + 3c_1(\mathcal{O})) = \varphi^*(c_1(B) - c_1(\mathcal{L})) \quad .$$

It follows that Y is a Calabi-Yau if $c_1(\mathcal{L}) = c_1(B)$.

Concerning X , it is obtained as the double cover ramified over \underline{Q} ; it follows that $2c_1(X)$ agrees with the pull-back of $2c_1(B) - [Q]$, so $c_1(X) = 0$ if $2c_1(B) = [Q]$. As h is a section of \mathcal{L}^2 (see §3.5), this shows that X is a Calabi-Yau when $c_1(\mathcal{L}) = c_1(B)$.

contributions coming from world-volume fluxes located on the seven branes. If we ignore the world volume fluxes, the type IIB D3 tadpole induced by the D7 branes and the O7 plane is:

$$\text{Type IIB : } N_{D3} = \frac{1}{2} \left(\sum_i \frac{4\chi(O_i)}{24} + \sum_j \frac{\chi(D_j)}{24} \right).$$

In F-theory, the choice of the D7 branes is given by the geometry of the Calabi-Yau four-fold. The D3 tadpole induced by the 7-branes is given solely in terms of the Euler characteristic of the four-fold:

$$\text{F-theory : } N_{D3} = \frac{\chi(Y)}{24}.$$

Since the D3 branes are S-dual invariant, the D3-tadpole should be the same in F-theory and in type IIB. In the absence of fluxes, this gives a topological relation between the Euler characteristic of the four-fold and the Euler characteristics of the orientifold planes and the D7 branes. This is the *F-theory-type-IIB D3 tadpole matching relation* [25, 24]:

$$\text{F-theory-type IIB D3 matching : } 2\chi(Y) = 4 \sum_i \chi(O_i) + \sum_j \chi(D_j).$$

This relation has been checked to hold in the case of Sen's weak coupling of F-theory compactified on a Calabi-Yau four-fold given by a Weierstrass model (elliptic fibration of type E_8), once the singularities found in Sen's limit are taken into account as providing a contribution to the corresponding Euler characteristic [25, 24]. An F-theory-type IIB tadpole mismatch signals that one has to consider adding world-volume fluxes on the D7-branes. This is reviewed in [25].

Now that we have introduced several new weak coupling limits of F-theory, it is natural to check the validity of this relation. Since some of our limits lead to configurations involving only smooth divisors, the F-theory tadpole matching condition is even more constrained since there are no singularities providing contributions to the Euler characteristic to correct a possible mismatch.

An interesting aspect of the tadpole matching condition in the examples we have examined is that it follows from a Chern class identity largely independent of the specific hypotheses leading to it: it has been shown in the E_8 -case to hold for elliptic fibrations of any dimension and without imposing the Calabi-Yau condition, and it is valid at the level of Chern classes. We will see that all these properties hold as well for the E_6 and E_7 examples obtained in §3.

The left-hand side of the F-theory-type-IIB D3 tadpole matching relation involves the Euler characteristic of the elliptic fibration. This can be expressed solely in terms of the geometry of the base. A formula computing the Euler characteristic of an elliptic fibered four-fold was first given by Sethi-Vafa-Witten [9]. It was then extended to E_7 and E_6 fibrations by Klemm, Lian, Roan and Yau [35]. An equivalent formula for singular four-folds was obtained by Andreas and Curio [42]. In the E_8 case, the relation valid outside of the Calabi-Yau condition and at the level of Chern class was derived in [24].

In this section we will generalize Sethi-Vafa-Witten at the level of the total Chern class for elliptic fibrations of type E_6 , E_7 , E_8 of any dimension. The case of E_8 was already treated in [24]. We will then use the generalized Sethi-Vafa-Witten formula to prove the F-theory-type-IIB tadpole matching condition for the different limits we have obtained in the previous section. We will see that it holds for the smooth configurations in E_7 and E_6 ,

and also for the E_7 limits involving Whitney umbrella singularities. For the latter we use the Euler characteristic χ_o introduced in [24, 25] and its corresponding Chern class.

The new elliptic fibrations we consider here allow for configurations of smooth branes. In §4.4 we provide a theorem which classifies all possible types of smooth brane configurations satisfying the tadpole matching condition in a universal sense, for E_8 , E_7 , E_6 fibrations over a base of arbitrary dimension. In particular, we find that no such configurations can occur in the E_8 case, over an unrestricted base. We observe that restricting to the Calabi-Yau case in dimension 3 potentially allows for more types of configurations of smooth branes satisfying the tadpole relation.

4.2. Sethi-Vafa-Witten formulas. Let $Y \rightarrow B$ be an elliptic fibration of the kind considered in §2. Under the assumption that Y is a Calabi-Yau manifold, formulas for the Euler characteristic of Y may be found in [35], (3.11) and §§7 and 8; some of these formulas were also given in [9].

Proposition 4.2 ([9], [35]). *Let $Y \rightarrow B$ be an elliptic fibration of type E_6 , E_7 , E_8 , with Y a Calabi-Yau fourfold. Then*

$$\begin{cases} E_6 : & \chi(Y) = \int 12c_1(B)c_2(B) + 72c_1(B)^3 \\ E_7 : & \chi(Y) = \int 12c_1(B)c_2(B) + 144c_1(B)^3 \\ E_8 : & \chi(Y) = \int 12c_1(B)c_2(B) + 360c_1(B)^3 \end{cases}$$

Here $c_i(B)$ denotes the Chern class $c_i(TB)$ of the tangent bundle, and \int denotes degree in B . These formulas suffice as one ingredient in the verification of the relations arising from tadpole matching in the limits considered in this paper, in the physically more immediately significant case of Calabi-Yau fourfolds.

One point of our message is however that these relations, inspired by the physically significant cases, have a much wider range of validity. In order to realize this, we have to upgrade Proposition 4.2 to smooth fibrations involving varieties of arbitrary dimension, and for which Y is not necessarily a Calabi-Yau. Also, we have to produce identities at the level of total Chern classes; the Euler characteristic is just the degree of the piece of dimension zero in the total Chern class.

Surprisingly, the general formulas we obtain are in fact *simpler* than the formulas recalled in Proposition 4.2, in the sense that they have a more conceptual geometric formulation, and they do not directly involve random-looking coefficients. They extend directly the observation (hidden in the formulas of Proposition 4.2) that the Euler characteristic of a fibration Y as in §2 equals a fixed multiple of the Euler characteristic of the hypersurface $g = 0$ of B . In this formulation, the Calabi-Yau condition is irrelevant.

Theorem 4.3. *Let $\varphi : Y \rightarrow B$ be an elliptic fibration of type E_6 , E_7 , E_8 , as in §2. Let Z be a smooth hypersurface of B in the same class as $g = 0$ (with notation as in (1), (2), and (3)). Then*

$$\varphi_*(c(Y)) = m \cdot c(Z)$$

where $m = 4, 3, 2$, resp. for Y of type E_6 , E_7 , E_8 , resp.

A straightforward computation shows that Theorem 4.3 implies the formulas given in Proposition 4.2; for this, use that $\int \varphi_*(c(Y)) = \int c(Y) = \chi(Y)$ and $\int c(Z) = \chi(Z)$, the adjunction formula, and Proposition 4.1.

Remark 4.4. The ingredients appearing in Theorem 4.3 admit the following compelling geometric description. The fibrations considered here have $m - 1$ distinguished sections, obtained by intersecting with $z = 0$ the loci specified by (1), (2), (3). Over the divisor Z with equation $g = 0$ there is in fact one more section, corresponding to the point $(z : x : y) = (1 : 0 : 0)$ in each fiber. The content of Theorem 4.3 is that the complement of these m sections of Z in Y contributes 0 to the push-forward of $c(Y)$. This is intriguing, because the fibers of the projection from this complement to Y do not all have vanishing Euler characteristic.

Proof of Theorem 4.3. This is again a relatively straightforward computation, using adjunction and standard intersection-theoretic calculus. We will sketch the E_6 case, as an illustration. Recall that Y is defined by equation (1) in $\mathbb{P}(\mathcal{O} \oplus \mathcal{L} \oplus \mathcal{L})$. Denote by π the projection from this bundle to B ; also, denote by L, H , resp., the classes $c_1(\mathcal{L}), c_1(\mathcal{O}(1))$, resp., and their pull-backs. Standard arguments give

$$c(Y) = \frac{(1+H)(1+L+H)^2}{1+3H+3L}(3H+3L)\pi^*(c(B))$$

as a class in $\mathbb{P}(\mathcal{O} \oplus \mathcal{L} \oplus \mathcal{L})$, and hence by the projection formula

$$\varphi_*(c(Y)) = \pi_* \left(\frac{(1+H)(1+L+H)^2}{1+3H+3L}(3H+3L) \right) c(B) \quad .$$

On the other hand, g is a section of \mathcal{L}^3 in the E_6 case; thus

$$c(Z) = \frac{3L}{1+3L} c(B) \quad .$$

Thus, to prove the statement in the E_6 case it suffices to show that

$$(24) \quad \pi_* \left(\frac{(1+H)(1+L+H)^2}{1+3H+3L}(3H+3L) \right) = 4 \cdot \frac{3L}{1+3L} \quad .$$

Again by the projection formula, performing this verification amounts to computing the push forwards $\pi_*(H^i)$. For these, note that

$$\pi_*(1+H+H^2+\cdots) = s(\mathcal{O} \oplus \mathcal{L} \oplus \mathcal{L}) = \frac{1}{(1+L)^2} \cap [B] = (1-2L+3L^2-4L^3+\cdots) \cap [B] :$$

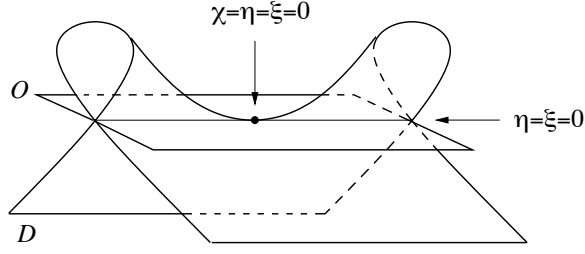
the first equality holds by definition of Segre class (§3.1 in [41]), and the second holds because the Segre class is the inverse of the Chern class (§3.2 in [41]). Matching terms of like dimension, we see that π_* acts as follows:

$$1 \mapsto 0; \quad H \mapsto 0; \quad H^2 \mapsto 1; \quad H^3 \mapsto -2L; \quad H^4 \mapsto 3L^2; \quad \text{etc.}$$

This reduces (24) to an elementary verification.

The proofs in the E_7 and E_8 case follow the same pattern⁸. □

⁸In [24] we gave a different argument for the E_8 case, based on the study of the explicit contributions of singular fibers.

FIGURE 10. Sen's E_8 limit

4.3. Euler characteristic and Chern class identities. We now move on to the verification of the tadpole relation for the limits considered in §3. The E_8 case of Sen's limit is treated in detail in [24], and we briefly review the result here for the convenience of the reader. The second E_7 limit encountered in §3.3 has similarities with Sen's from the geometric point of view; we will show that the same notion of Euler characteristic (and Chern class) used in §4.3.1 leads to a correct identity in this case. For the other two limits obtained in §3 the support of the branes is nonsingular, so the verification of the identities is (even) more straightforward.

The identities involve the fibration Y and hypersurfaces in the double cover X of B ramified along O ; we take $h = \xi^2$ as an equation for X in the total space of \mathcal{L} ; $\xi = 0$ defines the zero section in the total space, and the ramification locus O on X . The orientifold in the theory is supported on O . The various branes are supported on the other components D of the preimage of the limiting discriminant Δ_h .

4.3.1. *Sen's E_8 limit.* Pulling back the equation of Δ_h to X gives

$$\xi^4(\eta^2 + 12\xi^2\chi) \quad ;$$

we find one $D7$ -brane D supported on the hypersurface $\eta^2 + 12\xi^2\chi = 0$. This is a singular variety, with a Whitney umbrella structure along the singular locus $\eta = \xi = 0$, pinched along $\chi = \eta = \xi = 0$ (see Figure 10): thus, D is a Whitney $D7$ brane. In [24] we prove that

$$2\chi(Y) = 4\chi(O) + \chi_o(D) \quad ,$$

where $\chi_o(D)$ is defined as the Euler characteristic of the normalization \bar{D} of D , corrected by a contribution of the pinch locus S . More precisely ([24], Corollary 4.7),

$$(25) \quad 2\chi(Y) = 4\chi(O) + \chi(\bar{D}) - \chi(S) \quad ;$$

in the case $\dim B = 3$, the locus S consists of isolated points, and $\chi(S)$ is simply the number of such points. However, (25) holds regardless of the dimension of B . In fact, (25) is just the degree of the term of dimension 0 in an identity involving the total Chern classes of these loci:

$$(26) \quad 2\varphi_*(c(Y)) = 4\rho_*(c(O)) + \pi_*(c(\bar{D})) - i_*(c(S)) \quad ,$$

where the push-forwards all bring the named classes to the homology of B ([24], Theorem 4.6).

4.3.2. *The $\Delta_{112} \rightarrow \Delta_{13} E_7$ limit.* The limiting configuration for the second E_7 limit obtained in §3.3 has points of similarity with Sen's limit. In this case, Δ_h is defined by (19),

$$h^2(h - 4k^2)(\phi^2 - h\gamma) \quad ,$$

and hence it pulls back to

$$\xi^4(\xi - 2k)(\xi + 2k)(\phi^2 - \xi^2\gamma) \quad .$$

Thus, we find the orientifold O , together with a brane D_1 splitting into a brane-image-brane, and a Whitney D7-brane D_2 . The situation is analogous to that in Sen's limit, but two additional smooth hypersurfaces D_{1+} , D_{1-} are present, which are interchanged by the symmetry $\xi \mapsto -\xi$. Note that these two hypersurfaces are in the same class as ξ .

Claim 4.5. $2\chi(Y) = 4\chi(O) + \chi(D_{1+}) + \chi(D_{1-}) + \chi_o(D_2) \quad .$

Here, $\chi_o(D_2)$ is defined in precisely the same fashion as in Sen's limit. The Euler characteristics of D_{1+} and D_{1-} are ordinary Euler characteristics, since these components are smooth. They in fact equal $\chi(O)$.

Claim 4.5 is obtained by taking the degree of the term of dimension 0 in the following identity of Chern classes, which holds in arbitrary dimension:

$$(27) \quad 2\varphi_*(c(Y)) = \rho_*(4c(O) + c(D_+) + c(D_-)) + \pi_*(c(\overline{D})) - i_*(c(S)) \quad ,$$

where again S denotes the pinch locus, and the push-forwards map the classes to the homology of B .

To verify this identity, first note O , D_+ , and D_- are smooth and have the same class in X ; thus $4c(O) + c(D_+) + c(D_-) = 6c(O)$. Since O maps isomorphically to \underline{O} in B ,

$$\rho_*(4c(O) + c(D_+) + c(D_-)) = 6c(\underline{O}) = 6 \cdot \frac{2L}{1+2L} \cdot c(B) \quad .$$

Concerning the other terms, the normalization \overline{D} of the Whitney umbrella maps generically 2-to-1 onto the corresponding component \underline{D}' of Δ_h , with equation

$$\phi^2 - h\gamma = 0 \quad ,$$

and maps 1-to-1 over the pinch locus S . It follows that

$$\pi_*(c(\overline{D})) - i_*(c(S)) = 2c_{\text{SM}}(\underline{D}') - 2c(S) \quad ,$$

where $c_{\text{SM}}(\underline{D}')$ is the Chern-Schwartz-MacPherson class of \underline{D}' (see §4.2 of [24]). The class $c_{\text{SM}}(\underline{D}')$ is computed in Lemma 4.4 of [24]; considering that \underline{D}' has class $6L$, and the class of S is $(2L)(3L)(4L)$, we get

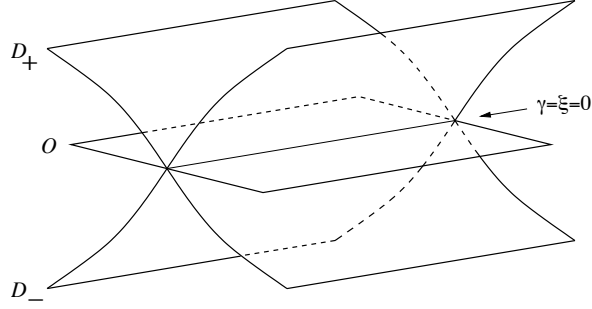
$$c_{\text{SM}}(\underline{D}') = \left(\frac{6L}{1+6L} - \frac{1}{1+6L} \frac{(2L)(3L)(4L)}{(1+2L)(1+3L)(1+4L)} \right) c(B) \quad ,$$

and hence $\pi_*(c(\overline{D})) - i_*(c(S))$ equals

$$(28) \quad 2 \left(\frac{6L}{1+6L} - \frac{1}{1+6L} \frac{(2L)(3L)(4L)}{(1+2L)(1+3L)(1+4L)} \right) c(B) - 2 \frac{(2L)(3L)(4L)}{(1+2L)(1+3L)(1+4L)} c(B) \\ = \frac{12L}{(1+2L)(1+4L)} c(B)$$

Summarizing, the right-hand side of (27) equals

$$(29) \quad 6 \cdot \frac{2L}{1+2L} c(B) + \frac{12L}{(1+2L)(1+4L)} c(B) = \frac{24L}{1+4L} c(B) \quad .$$

FIGURE 11. E_7 limit, $\Delta_{22} \rightarrow \Delta_4$

On the other hand, Theorem 4.3 shows

$$\varphi_*(c(Y)) = 3 \cdot c(Z) \quad ,$$

where Z is defined by $g = 0$, and hence has class $4L$. Thus, the left-hand side of (27) is

$$(30) \quad 2 \cdot 3 \cdot \frac{4L}{1+4L} c(B) \quad .$$

The expressions (29) and (30) match, completing the proof of (27) and verifying Claim 4.5.

4.3.3. *The $\Delta_{22} \rightarrow \Delta_4$ E_7 limit.* The first limit obtained in §3.3 has a simpler geometric description. The limiting discriminant is defined by (18):

$$h^2 (\gamma^2 - \phi^2 h)$$

and pulls back on X to

$$\xi^4 (\gamma + \phi\xi) (\gamma - \phi\xi) \quad .$$

In this case, the whole brane contribution to the configuration is split into an image-brane-image pair. We let D_+ , D_- denote these two components. All three components O , D_+ , D_- are smooth, of class L , $4L$, $4L$ respectively. The hypersurfaces D_+ and D_- are tangent to each other along $\xi = \gamma = \phi = 0$, and otherwise meet transversally.

Claim 4.6. $2\chi(Y) = 4\chi(O) + \chi(D_+) + \chi(D_-)$.

Again, this identity is just a manifestation of an identity of Chern classes, holding in any dimension and without any Calabi-Yau restriction:

$$(31) \quad 2\varphi_*(c(Y)) = \rho_*(4c(O) + c(D_+) + c(D_-)) \quad .$$

Verifying (31) is essentially straightforward. Since O maps isomorphically to \underline{O} ,

$$\rho_*c(O) = c(\underline{O}) = \frac{2L}{1+2L}c(B) \quad .$$

Each of D_+ and D_- is a smooth hypersurface in X , of class $4L$, hence

$$c(D_{\pm}) = \frac{4L}{1+4L}c(X) = \frac{4L}{1+4L} \cdot \frac{1+L}{1+2L} \cdot \rho^*(c(TB)) \cap [X] \quad .$$

By the projection formula:

$$(32) \quad \rho_* c(D_{\pm}) = \frac{4L}{1+4L} c(X) = \frac{4L(1+L)}{(1+2L)(1+4L)} c(TB) \cap (2[B]) \\ = \frac{8L(1+L)}{(1+2L)(1+4L)} c(B) \quad .$$

Therefore, the right-hand side of (31) equals

$$\left(4 \cdot \frac{2L}{1+2L} + 2 \cdot \frac{8L(1+L)}{(1+2L)(1+4L)} \right) c(B) = \frac{24L}{1+4L} c(B) \quad .$$

This equals the left-hand side by Theorem 4.3 (cf. (30)), completing the verification.

4.3.4. *The $\Delta_Q \rightarrow \Delta_P E_6$ limit.* Our last example is the E_6 limit found in §3.4. The limiting discriminant is defined by (23):

$$h^2(h+3k^2)(\gamma^2 - h\phi^2) \quad .$$

and pulls back to

$$\xi^4(\gamma + \xi\phi)(\gamma - \xi\phi)(\xi + i\sqrt{3}k)(\xi - i\sqrt{3}k) \quad .$$

This configuration consists of the orientifold O and of *two* brane-image-brane pairs: a first pair $D_{1\pm}$, with components of class $3L$, and a second pair $D_{2\pm}$, with components of class L . The second pair is transversal, while D_{1+} and D_{1-} are tangent along $\xi = \gamma = \phi = 0$.

Claim 4.7. $2\chi(Y) = 4\chi(O) + \chi(D_{1+}) + \chi(D_{1-}) + \chi(D_{2+}) + \chi(D_{2-}) \quad .$

Once more, this identity of Euler characteristics is simply a numerical avatar of a general identity of Chern classes, which holds in arbitrary dimension and regardless of Calabi-Yau restrictions:

$$(33) \quad 2\varphi_*(c(Y)) = \rho_*(4c(O) + c(D_{1+}) + c(D_{1-}) + c(D_{2+}) + c(D_{2-})) \quad .$$

The verification of (33) follows the same guidelines as the verification of (31) given above. Since O , $D_{2\pm}$ are smooth hypersurfaces of the same class, mapping isomorphically to \underline{Q} ,

$$\rho_*(4c(O) + c(D_{2+}) + c(D_{2-})) = 6\rho_*(c(O)) = 6 \cdot \frac{2L}{1+2L} c(B) \quad .$$

The components $D_{1\pm}$ have class $3L$ in X , and their contribution can be computed by the same method used for D_{\pm} in §4.3.3: this gives

$$\rho_* c(D_{1\pm}) = \frac{3L(1+L)}{(1+2L)(1+3L)} c(TB) \cap (2[B]) = \frac{6L(1+L)}{(1+2L)(1+3L)} c(B) \quad .$$

Therefore, the right-hand side of (33) equals

$$(34) \quad \left(6 \cdot \frac{2L}{1+2L} + 2 \cdot \frac{6L(1+L)}{(1+2L)(1+3L)} \right) c(B) = \frac{24L}{1+3L} c(B) \quad .$$

By Theorem 4.3, the left-hand side of (33) equals

$$\varphi_*(c(Y)) = 4 \cdot c(Z) \quad ,$$

where Z is given by $g = 0$. In the E_6 case g is a section of \mathcal{L}^3 , so this gives

$$2\varphi_*(c(Y)) = 2 \cdot 4 \cdot \frac{3L}{1+3L}$$

with the same result as (34), concluding the verification.

4.4. A classification of configurations of smooth branes. The method used in §4.3 to verify the tadpole relations can be used to explore the set of possible orientifold/brane configurations satisfying the tadpole relation, under the assumption that the supports of all branes are *nonsingular*.

For this, we propose the Ansatz that the tadpole relation, while originally obtained under specific hypotheses satisfied in the motivating physical setting, reflects a *universal* identity, holding regardless of the specific choice of L and of any restriction posed on the nonsingular base variety B . This is the case in the examples examined in §4.3. While the original tadpole relation is a specific statement about the geometry of Calabi-Yau fibrations, the universal tadpole relation is a formal identity of Euler characteristics, computed as functions of a variable L and of the Chern classes $c_1(B), c_2(B), \dots$ of the base.

The verifications carried out in §4.3 show that the tadpole relation holds universally in the examples obtained in §3. In the $\Delta_{22} \rightarrow \Delta_4 E_7$ case and in the $\Delta_Q \rightarrow \Delta_P E_6$ case, the branes are supported on *nonsingular* components of the limiting discriminant. We can ask whether there are other such ‘nonsingular’ configurations satisfying the universal tadpole relation. In the other two situations encountered in §4.3, a *singular* brane appears. Is this a necessity, or a pathology?

Informally, we find the following:

- Claim 4.8.**
- *There are no configurations of smooth branes satisfying the universal tadpole relation for E_8 fibrations;*
 - *The only configuration of smooth branes satisfying the universal tadpole relation for E_7 fibrations is the one arising from the $\Delta_{22} \rightarrow \Delta_4$ specialization, examined in §4.3.3;*
 - *The only configuration of smooth branes satisfying the universal tadpole relation for E_6 fibrations is the one arising from the $\Delta_Q \rightarrow \Delta_P$ specialization, examined in §4.3.4.*

Thus, the appearance of the singular $D7$ -brane in Sen’s limit and in the E_7 limit studied in §4.3.2 is not accidental.

Note that the Calabi-Yau condition is not used in this statement. It is interesting to study configurations that satisfy the tadpole relation universally but subject to a Calabi-Yau hypothesis; this narrows the scope of the tadpole relation, so it can potentially be satisfied by more configurations. We will discuss this case at the end of the section.

We formalize Claim 4.8 as follows. We consider configurations of (not necessarily distinct) hypersurfaces D_1, \dots, D_r of the double cover X of B ramified along O . We assume that D_i has class $a_i L$, and that $\sum a_i = 12$: this is the case if the divisors appear as components of a limit discriminant. Typically, the orientifold $\xi = 0$ corresponds to 4 components D_i , with $a_i = 1$, but we do not impose this as a necessary condition.

Assume all hypersurfaces D_i are nonsingular. A strong tadpole relation then takes the form

$$(35) \quad 2\varphi_*c(Y) = \sum_{i=1}^r \rho_*(c(D_i)) \quad .$$

Again, typically $D_1 = D_2 = D_3 = D_4$ would be the support of the orientifold O , so this relation, after taking degrees, would amount to

$$(36) \quad 2\chi(Y) = 4\chi(O) + \sum_{i>4} \chi(D_i) \quad ,$$

the ordinary tadpole relation. Applying Theorem 4.3, (35) may be rewritten

$$(37) \quad 2m c(Z) = \sum_{i=1}^r \rho_*(c(D_i)) \quad ,$$

where Z is a nonsingular hypersurface in B , of class aL . We have $(m, a) = (2, 6), (3, 4), (4, 3)$ resp. in the E_8, E_7, E_6 case, resp. We say that (37) is ‘universally satisfied’ if the corresponding identity depending on a, a_i is satisfied as a formal identity of Chern classes, independently of the choice of L or B .

The precise version of Claim 4.8 is as follows.

Theorem 4.9. *Assume all hypersurfaces D_i are nonsingular, and D_i has class $a_i L$, with $a_i > 0$ integers and $\sum_i a_i = 12$; assume Z is also nonsingular, and has class aL . Then (37) is universally satisfied only in the following three cases:*

(m, a)	(a_1, a_2, \dots)
$(3, 4)$	$(1, 1, 1, 1, 4, 4)$
$(4, 3)$	$(1, 1, 1, 1, 1, 1, 3, 3)$
$(6, 2)$	$(1, \dots, 1)$

In fact, the weaker requirement that (36) is universally satisfied for $\dim B = 3$ suffices to draw the same conclusion.

The first and second case reproduce the configurations appearing in §4.3.3 and 4.3.4: the orientifold (of class L) appears with multiplicity 4 in both cases; in the E_7 case, a brane-image-brane appears with components of class $4L$; in the E_6 case, two brane-image-brane pairs appear, of class L and $3L$, respectively.

No case corresponding to E_8 fibrations appears in the list. We do not have a geometric interpretation for the third case displayed in Theorem 4.9.

To prove Theorem 4.9, rewrite (37) in terms of L and $c(B)$: by essentially the same arguments used in §4.3, this yields

$$(38) \quad m \cdot \frac{aL}{1 + aL} = \left(\sum_{i=1}^r \frac{a_i L}{1 + a_i L} \right) \frac{1 + L}{1 + 2L}$$

up to a common factor of $c(B)$, which may be discarded as the identity is required to hold universally. For the same reason, (38) must hold as an identity of rational functions in the indeterminate L . Theorem 4.9 is proved by verifying that (38) is satisfied in this sense only in the three cases listed in the statement.

In fact, requiring that $\sum_i a_i = 12$, multiplying both sides of (38) by $c(B)$, and imposing a match in degree 3 leads to precisely the same list of cases. Thus, the weaker requirement that the tadpole relation should be universally satisfied at the level of Euler characteristics for $\dim B = 3$ (in the form (36)) constrains the situation in precisely the same way.

Carrying out this last verification under the additional assumption that $L = c_1(TB)$ explores the possible configurations in the more physically significant Calabi-Yau case

(cf. Proposition 4.1). This produces three more possibilities:

(m, a)	(a_1, a_2, \dots)
(2, 6)	(1, 1, 1, 1, 1, 7)
(3, 4)	(1, 1, 1, 1, 1, 1, 5)
(4, 3)	(1, 2, 2, 2, 2, 3)

The first case is the E_8 configuration described in [24], §3. We stress that these configurations satisfy the tadpole relation only in the Calabi-Yau case; this is a weaker requirement than that imposed in Theorem 4.9.

It would be interesting to provide a geometric realization of the third configuration listed in Theorem 4.9.

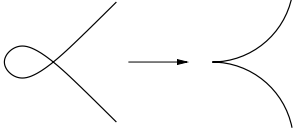
5. A VISIT TO THE ZOO

The requirement that $j \propto h^4$ adopted in §3 corresponds to a pure O7 orientifold plane with no D7-brane on top of it. As we have observed at the end of §3.5, this requirement may be weakened to $j \propto h^{4-n}$ for $0 \leq n \leq 4$, in order to accommodate bound states of the orientifold plane with n pairs of D7 brane-image-brane on top of it. These configurations also lead to Chern class identities. For example the E_6 limit presented in §1.8.3 and constructed in detail in §3.4 specializes to a configuration with $j \propto h^3$ when $k = 0$. Indeed, in that case the D7 brane-image-brane $D_{2\pm} : \xi \pm i\sqrt{3}k = 0$ reduces to $D_{2\pm} : \xi = 0$ and therefore they are wrapping the same locus as the orientifold plane. This explains the behavior $j \propto h^3$.

There are other mechanisms producing different limits, corresponding to different ways to satisfy the generality hypothesis (often by introducing terms with higher C -weight). Such operations can often be interpreted as specializations of other known limits, and change the underlying geometry in a controlled fashion. Again, it is often possible to provide a physical interpretation for the resulting configurations. However, limits arising in this way are often necessarily non-supersymmetric. For example, the very last limit listed below is obtained by killing a first-order perturbation term. This results in a configuration of smooth branes which in general does not satisfy the F-theory-type IIB tadpole matching condition.

Here we simply list several families $Y_h(C)$, with the corresponding leading order in j . The discriminant can be recovered from the j -invariant. If the j -invariant is given as an irreducible fraction $j \sim \frac{h^{4-n}}{C^r \Delta^l}$, the discriminant is recovered as $\Delta = h^{2+n} \Delta'$. Note that several limits in the list presented here do not satisfy the double intersection properties.

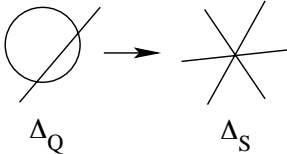
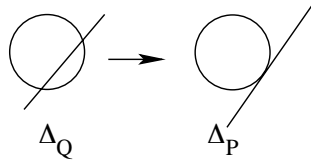
5.1. E_8 limits.

Type	Realization	j -invariant
	$f = -3h^2 + C\phi$ $g = -2h^3 + C\gamma$	$\frac{1}{C} \cdot \frac{h^3}{h\phi - \gamma}$
	$f = -3h^2 + C\phi$ $g = -2h^3 + Ch\phi + C^3\gamma$	$\frac{1}{C^2} \cdot \frac{h^4}{\phi^2}$

5.2. E_7 limits.

Type	Realization	j -invariant
	$e = h$ $f = C\phi$ $g = C\gamma$	$\frac{1}{C} \cdot \frac{h^2}{\gamma}$
	$e = h$ $f = 2C\phi$ $g = C^2\gamma$	$\frac{1}{C^2} \cdot \frac{h^3}{h\gamma - \phi^2}$
	$e = -2h$ $f = Ch\eta + C^2\phi$ $g = h^2 + Ch^2 + C^2\gamma$	$\frac{1}{C^2} \cdot \frac{h}{(h - \eta^2)}$
	$e = -2h$ $f = Ch\eta + C^2\phi$ $g = h^2 + C\gamma$	$\frac{1}{C^2} \cdot \frac{h^4}{(\eta^2 h^3 - \gamma^2)}$
	$e = 2h$ $f = C^2\phi$ $g = h^2 + C\gamma$	$\frac{1}{C^2} \cdot \frac{h^4}{\gamma^2}$
	$e = 4h - 6k^2$ $f = 8k(h - k^2) + Ch\eta + C^2\phi$ $g = k^2(4h - 3k^2) + Ch^2 + C^2\gamma$	$\frac{1}{C} \cdot \frac{h^3}{(h - k^2)(h - k\eta)}$
	$e = 4h - 6k^2$ $f = 8k(h - k^2) + C\phi$ $g = k^2(4h - 3k^2) + Ch^2 + C^2\gamma$	$\frac{1}{C} \cdot \frac{h^3}{(h - k^2)(h^2 - k\phi)}$
	$e = 4h - 6k^2$ $f = 8k(h - k^2) + Ch\eta + C^2\phi$ $g = k^2(4h - 3k^2) + C\gamma$	$\frac{1}{C} \cdot \frac{h^3}{(h - k^2)(\gamma - kh\eta)}$
	$e = 4h - 6k^2$ $f = 8k(h - k^2) + C\phi$ $g = k^2(4h - 3k^2) + C\gamma$	$\frac{1}{C} \cdot \frac{h^3}{(h - k^2)(\gamma - k\phi)}$
	$e = 4h - 6k^2$ $f = 8k(h - k^2) + C\phi$ $g = k^2(4h - 3k^2) + C^3\gamma$	$\frac{1}{C} \cdot \frac{h^3}{k\phi(h - k^2)}$
	$e = 4h - 6k^2$ $f = 8k(h - k^2) + C\phi$ $g = k^2(4h - 3k^2) + Ck\phi + C^3\gamma$	$\frac{1}{C^2} \cdot \frac{h^4}{\phi^2(h - k^2)}$

5.3. E_6 limits.

Type	Realization	j -invariant
	$d = C\delta$ $e = 3h$ $f = 3h + C\phi$ $g = C\delta h + C^2\gamma$	$\frac{1}{C^2} \cdot \frac{h^2}{\phi^2}$
	$d = C\delta$ $e = 3h$ $f = 3h + C\phi$ $g = C(\delta + \eta)h + C^2\gamma$	$\frac{1}{C^2} \cdot \frac{h^2}{\phi^2 - h\eta^2}$
	$d = C\delta$ $e = 3h$ $f = 3h + C\phi$ $g = C(h\delta + \gamma)$	$\frac{1}{C^2} \cdot \frac{h^3}{\gamma^2 - h\phi^2}$
	$d = 6k$ $e = 9k^2 + 3h$ $f = 9k^2 + 3h + C\phi$ $g = 2k(5k^2 + 3h) + C(h\eta + k\phi) + C^2\gamma$	$\frac{1}{C^2} \cdot \frac{h^3}{(h\eta^2 - \phi^2)(h + 3k^2)}$
	$d = 6k$ $e = 9k^2 + 3h$ $f = 9k^2 + 3h + C^2\phi$ $g = 2k(5k^2 + 3h) + C\gamma$	$\frac{1}{C^2} \cdot \frac{h^4}{\gamma^2(h + 3k^2)}$
	$d = 6k$ $e = 9k^2 + 3h$ $f = 9k^2 + 3h + C^2\phi$ $g = 2k(5k^2 + 3h) + C(h\eta + k\phi) + C^2\gamma$	$\frac{1}{C^2} \cdot \frac{h^4}{(h + 3k^2)(h\eta + k\phi)^2}$
	$d = 6k$ $e = 9k^2 + 3h$ $f = 9k^2 + 3h + C\phi$ $g = 2k(5k^2 + 3h) + C^2\gamma$	$\frac{1}{C^2} \cdot \frac{h^4}{\phi^2(h + 3k^2)(h - k^2)}$

6. CONCLUSIONS AND DISCUSSIONS

In this paper, we have constructed new type IIB orientifold weak coupling limits of F-theory. This was done by considering elliptic fibrations which are not in Weierstrass form. The derivation of the limits was streamlined by first introducing a geometric interpretation of Sen’s weak coupling limit in terms of a transition from semistable singular fibers to unstable singular fibers. This leads to a simple algorithm to construct new limits from new families of elliptic fibrations. We would like to conclude with a discussion on different issues raised by the existence of the new weak coupling limits and with a look at future directions.

New F-theory lift of type IIB and F-theory geometric engineering. The new weak coupling limits presented in this paper can be used ‘in reverse’ as different possible F-theory lifts for type IIB orientifold compactifications. This provides new tools for model builders. The geometric intuition behind the construction of a given weak coupling limit is a valuable asset for F-theory geometric engineering. Since each limit comes with a natural brane spectrum, one can avoid intricate geometric tunings by starting with a family that will more naturally lead to a brane spectrum close to the one we would like to get in type IIB. For example, Sen’s weak coupling limit of a Weierstrass model favors type IIB configurations where branes recombined into a unique irreducible and singular component, which we refer to as a ‘Whitney D7-brane’ since its singularities are reminiscent of the Whitney umbrella $u^2 - v^2w = 0$ in \mathbb{C}^3 . Naively, one might therefore conclude that F-theory does not at all favor brane-image-brane pairs, in contrast to assumptions generally made in the type IIB orientifold literature not related to F-theory [43]. However, the existence of new weak coupling limits shows that Sen’s limit is not the unique weak coupling limit of F-theory and other limits might allow supersymmetric brane-image-brane configurations. This is exactly the case of elliptic fibrations of type E_6 and E_7 since they naturally favors smooth brane-image-brane pairs as illustrated in §1.8. The D-brane deconstruction point of view [25], which is based on K-theory and is independent of taking a weak coupling limit of F-theory, gives the general structure of D7-brane singularities. Brane-image-brane pairs and Whitney D7-branes are just particular realizations of this general structure.

F-theory away from Weierstrass models. Since any elliptic fibration is associated by means of a birational transformation to a Weierstrass model, each of the new limits presented here leads to a new weak coupling limit for a Weierstrass model as well. However, the resulting Weierstrass model is not necessarily smooth; its Euler characteristic is different from the Euler characteristic of the (smooth) fibration it is modeling, and also different from the Euler characteristic of a smooth E_8 fibration on the same base and endowed with the same line bundle. In particular, for F-theory compactified on a four-fold this implies that all these models will in general have different D3 tadpoles. Elliptic fibrations which are not in Weierstrass form have to be considered as physically different, and interesting in their own right. For example, we show that supersymmetric brane-image-brane configurations are allowed in F-theory for smooth E_6 and E_7 elliptic fibrations whereas they are generally excluded for smooth Weierstrass models.

F-theory-type-IIB D3 tadpole matching. The duality between type IIB and F-theory requires that the D3 tadpole is the same in both theory since D3 branes are invariant under S-duality. In the absence of fluxes, this leads to a simple relation between the Euler characteristics of the four-fold and of the divisors on which the branes and orientifold planes

are wrapped. As explained in [25], this relation can be used as an indication for turning on world volume fluxes for certain configuration of D-branes for which the F-theory-type-IIB D3 tadpole matching does not hold in the absence of fluxes. However, such fluxes can induce a violation of the D-term constraints, for example for a brane-image-brane pair except if the pair coincides with the orientifold plane. For this reason, brane-image-brane pairs in Sen's limit of a Weierstrass model are generally non-supersymmetric [25] since they require fluxes to satisfy the F-theory-type IIB D3 tadpole relation. Here, we have constructed limits leading to supersymmetric brane-image-brane configurations. This was only possible by considering families for which the F-theory-type-IIB D3 tadpole matching relation holds without any need for fluxes, thanks to the fact that the Euler characteristic of these elliptic fibrations (as computed in Proposition 4.2, for $c_1(B)^3 > 0$) is lower than the one of a smooth Weierstrass model constructed on the same base (in dimension 3, if $c_1(B)^3 > 0$). This is a simple example on how the choice of an appropriate family of elliptic fibrations is an important ingredient in the definition of a F-theory lift of a type IIB orientifold compactification.

Singular branes and the Euler characteristic χ_o . Several of the limits we have constructed here admit only branes wrapping smooth divisors in contrast to the case of Sen's limit of a general Weierstrass model, which generally leads to singular divisors of the Whitney umbrella type. We have also obtained a configuration that mixes a Whitney brane and smooth brane-image-brane pairs. We have explicitly checked that when the divisor is singular, the Euler characteristic χ_o introduced in [25, 24] is the appropriate one to use since it ensures the matching of the D3 tadpole in type IIB and in F-theory. We have presented a list of all smooth configurations that would satisfy the F-theory-type-IIB D3 tadpole relation. Several elements of that list have been constructed in this paper, but others have not, suggesting that there are still interesting weak coupling limit to be discovered.

Double intersection property and D-brane motion. The new limits presented here (in §5) have some intersection properties that do not match those of Sen's limit. For example, one would expect a D-brane to intersect an orientifold with even multiplicity. This is always the case for Whitney D7 branes, the typical example being Sen's limit of a Weierstrass model. The double intersection property also holds for brane-image-brane pairs. The double intersection property is supported by a probe argument which would imply that it should always hold for $O7^-$ branes characterized by having a negative D7 charge and orthogonal gauge group, when a stack of branes is on top of them [25]. However, several of the limits listed in §5 do not satisfy this property. Shall we disregard such limits or do they correspond to some exotic type of branes and/or orientifold planes? Another aspect of Sen's limit of a Weierstrass model is that the motion of the D7 branes is obstructed by the structure of the singularities of the D7 brane locus [26, 25]. Such obstructions are less severe in E_6 and E_7 elliptic fibrations since one can have smooth brane configurations.

String dualities and the structure of elliptic fibrations. The F-theory-type-IIB D3 tadpole matching is inspired by string theory duality. However, the corresponding relation between Euler characteristics is true in a more general context than its origin might indicate. We have shown that for each family we have considered there is a generalization of the F-theory-type-IIB D3 tadpole matching condition valid at the level of the total Chern classes and independent from the dimension of the base and the Calabi-Yau condition. In fact, in

all the examples we have examined, when the tadpole relation holds it does so as a formal identity in the Chern classes of the base and of the chosen line bundle, independent of finer geometric features of the varieties involved in the limit.

Open questions and future directions. There are several aspects of the constructions presented here that beg for additional analysis. For example, one would like to know if all the smooth configurations presented in §4.4, which satisfy the F-theory -type-IIB D3 tadpole matching condition, can be realized by a weak coupling limit. It would also be interesting to enlarge the possible F-theory lift of a type IIB configuration by studying other families of elliptic fibrations than the E_8 , E_7 and E_6 families studied here. For example, the family of elliptic fibration of type D_5 in the notation of [35] would be a natural starting point. It would also be important to determine the relevance of the limits which lead to brane configurations which do not satisfy the double intersection property that requires that a D7 brane always have a double intersection with an $O7^-$ orientifold plane. We note that a careful classification of all types of orientifold planes has been announced in [44]. It is clear that the D3 tadpole is not preserved by birational transformations since the Euler characteristic can change if one of the elliptic fibrations is singular or is not a Calabi-Yau. It would be interesting to study the possible gauge groups associated with each family. In particular, a discussion of the presence of exceptional groups for families that are not in Weierstrass form would be interesting in view of their central role of exceptional groups in F-theory local model building of Grand Unified Theories (GUTs).

Acknowledgments. P.A. thanks the Max-Planck-Institut für Mathematik in Bonn for the support in the month of July 2009, when most of this paper was written. He also thanks S.-T. Yau, F. Denef, and the Jefferson Laboratory at Harvard for the hospitality during a visit in May 2009, when this work was begun. M.E. would like to thank D. Bakary, F. Denef, A. Strominger, A. Tomasiello and S.-T. Yau for their support. He also thanks A. P. Braun, F. Denef, A. Klemm, H. Omer, A. Tomasiello, M. Wijnholt and H. Yavartanoo for interesting discussions. M.E. is partially funded by a DOE grant DE-FG02-91ER40654.

REFERENCES

- [1] C. Vafa, “Evidence for F-Theory,” *Nucl. Phys.* **B469** (1996) 403–418, arXiv:hep-th/9602022.
- [2] D. R. Morrison and C. Vafa, “Compactifications of F-Theory on Calabi–Yau Threefolds – I,” *Nucl. Phys.* **B473** (1996) 74–92, arXiv:hep-th/9602114.
- [3] D. R. Morrison and C. Vafa, “Compactifications of F-Theory on Calabi–Yau Threefolds – II,” *Nucl. Phys.* **B476** (1996) 437–469, arXiv:hep-th/960316.
- [4] J. H. Schwarz, “An $SL(2, Z)$ multiplet of type IIB superstrings,” *Phys. Lett.* **B360** (1995) 13–18, arXiv:hep-th/9508143 .
- [5] J. H. Schwarz, “The power of M theory,” *Phys. Lett.* **B367** (1996) 97–103, arXiv:hep-th/9510086 .
- [6] M. R. Douglas and M. Li, “D-Brane Realization of $N=2$ Super Yang-Mills Theory in Four Dimensions,” arXiv:hep-th/9604041.
- [7] A. Johansen, “A comment on BPS states in F-theory in 8 dimensions,” *Phys. Lett.* **B395** (1997) 36–41, arXiv:hep-th/9608186.
- [8] M. R. Gaberdiel and B. Zwiebach, “Exceptional groups from open strings,” *Nucl. Phys.* **B518** (1998) 151–172, arXiv:hep-th/9709013.
- [9] S. Sethi, C. Vafa, and E. Witten, “Constraints on low-dimensional string compactifications,” *Nucl. Phys.* **B480** (1996) 213–224, arXiv:hep-th/9606122.
- [10] F. Denef, “Les Houches Lectures on Constructing String Vacua,” arXiv:0803.1194 [hep-th].

- [11] R. Blumenhagen, V. Braun, T. W. Grimm, and T. Weigand, “GUTs in Type IIB Orientifold Compactifications,” *Nucl. Phys.* **B815** (2009) 1–94, arXiv:0811.2936 [hep-th].
- [12] C. Beasley, J. J. Heckman, and C. Vafa, “GUTs and Exceptional Branes in F-theory - I,” *JHEP* **01** (2009) 058, arXiv:0802.3391 [hep-th].
- [13] C. Beasley, J. J. Heckman, and C. Vafa, “GUTs and Exceptional Branes in F-theory - II: Experimental Predictions,” *JHEP* **01** (2009) 059, arXiv:0806.0102 [hep-th].
- [14] J. J. Heckman, A. Tavanfar, and C. Vafa, “The Point of E8 in F-theory GUTs,” arXiv:0906.0581 [hep-th].
- [15] J. J. Heckman and C. Vafa, “From F-theory GUTs to the LHC,” arXiv:0809.3452 [hep-ph].
- [16] R. Donagi and M. Wijnholt, “Model Building with F-Theory,” arXiv:0802.2969 [hep-th].
- [17] J. L. Bourjaily, “Local Models in F-Theory and M-Theory with Three Generations,” arXiv:0901.3785 [hep-th].
- [18] B. Andreas and G. Curio, “From Local to Global in F-Theory Model Building,” arXiv:0902.4143 [hep-th].
- [19] R. Blumenhagen, T. W. Grimm, B. Jurke, and T. Weigand, “F-theory uplifts and GUTs,” arXiv:0906.0013 [hep-th].
- [20] R. Donagi and M. Wijnholt, “Higgs Bundles and UV Completion in F-Theory,” arXiv:0904.1218 [hep-th].
- [21] J. Marsano, N. Saulina, and S. Schafer-Nameki, “F-theory Compactifications for Supersymmetric GUTs,” arXiv:0904.3932 [hep-th].
- [22] J. Marsano, N. Saulina, and S. Schafer-Nameki, “Monodromies, Fluxes, and Compact Three-Generation F-theory GUTs,” arXiv:0906.4672 [hep-th].
- [23] A. Sen, “Orientifold limit of F -theory vacua,” *Phys. Rev. D* (3) **55** (1997) no. 12, R7345–R7349. arXiv:hep-th/9702165.
- [24] P. Aluffi and M. Esole, “Chern class identities from tadpole matching in type IIB and F-theory,” *JHEP* **03** (2009) 032, arXiv:0710.2544 [hep-th].
- [25] A. Collinucci, F. Denef, and M. Esole, “D-brane Deconstructions in IIB Orientifolds,” *JHEP* **02** (2009) 005, arXiv:0805.1573 [hep-th].
- [26] A. P. Braun, A. Hebecker, and H. Triendl, “D7-Brane Motion from M-Theory Cycles and Obstructions in the Weak Coupling Limit,” *Nucl. Phys.* **B800** (2008) 298–329, arXiv:0801.2163 [hep-th].
- [27] I. Brunner and M. Herbst, “Orientifolds and D-branes in $N=2$ gauged linear sigma models,” arXiv:0812.2880 [hep-th].
- [28] A. Collinucci, “New F-theory lifts,” arXiv:0812.0175 [hep-th].
- [29] A. Collinucci, “New F-theory lifts II: Permutation orientifolds and enhanced singularities,” arXiv:0906.0003 [hep-th].
- [30] F. Denef, M. Esole, and M. Padi, “Orientiholes,” arXiv:0901.2540 [hep-th].
- [31] V. V. Batyrev, “Birational Calabi-Yau n -folds have equal Betti numbers,” in *New trends in algebraic geometry (Warwick, 1996)*, vol. 264 of *London Math. Soc. Lecture Note Ser.*, pp. 1–11. Cambridge Univ. Press, Cambridge, 1999.
- [32] P. Aluffi, “Chern classes of birational varieties,” *Int. Math. Res. Not.* (2004) no. 63, 3367–3377.
- [33] P. Aluffi, “Celestial integration, stringy invariants, and Chern-Schwartz-MacPherson classes,” in *Real and complex singularities*, Trends Math., pp. 1–13. Birkhäuser, Basel, 2007.
- [34] M. Bershadsky, K. A. Intriligator, S. Kachru, D. R. Morrison, V. Sadov and C. Vafa, “Geometric singularities and enhanced gauge symmetries,” *Nucl. Phys. B* **481**, 215 (1996) [arXiv:hep-th/9605200].
- [35] A. Klemm, B. Lian, S.-S. Roan, and S.-T. Yau, “Calabi-Yau four-folds for M- and F-theory compactifications,” *Nuclear Phys. B* **518** (1998) no. 3, 515–574. arXiv:hep-th/9701023.
- [36] A. Klemm, W. Lerche, and P. Mayr, “K3 Fibrations and heterotic type II string duality,” *Phys. Lett.* **B357** (1995) 313–322, arXiv:hep-th/9506112.
- [37] B. Andreas, G. Curio, and A. Klemm, “Towards the standard model spectrum from elliptic Calabi-Yau,” *Int. J. Mod. Phys. A* **19** (2004) 1987, arXiv:hep-th/9903052.
- [38] P. Berglund, A. Klemm, P. Mayr, and S. Theisen, “On type IIB vacua with varying coupling constant,” *Nucl. Phys.* **B558** (1999) 178–204, arXiv:hep-th/9805189.
- [39] A. Klemm, P. Mayr, and C. Vafa, “BPS states of exceptional non-critical strings,” arXiv:hep-th/9607139.

- [40] D. Husemöller, *Elliptic curves*, vol. 111 of *Graduate Texts in Mathematics*. Springer-Verlag, New York, second ed., 2004. With appendices by Otto Forster, Ruth Lawrence and Stefan Theisen.
- [41] W. Fulton, *Intersection theory*. Springer-Verlag, Berlin, 1984.
- [42] B. Andreas and G. Curio, “On discrete twist and four-flux in $N = 1$ heterotic/F- theory compactifications,” *Adv. Theor. Math. Phys.* **3** (1999) 1325–1413, arXiv:hep-th/9908193.
- [43] H. Jockers and J. Louis, “The effective action of D7-branes in $N = 1$ Calabi-Yau orientifolds,” *Nucl. Phys.* **B705** (2005) 167–211, arXiv:hep-th/0409098.
- [44] J. Distler, D. S. Freed, and G. W. Moore, “Orientifold Precs,” arXiv:0906.0795 [hep-th].